UQAR
Université du Québec
à Rimouski

Caractérisation des couches minces phytoplanctoniques et comparaison des mécanismes les affectant dans l'Estuaire Maritime du Saint-Laurent et dans la Baie de Monterey

Mémoire présenté

dans le cadre du programme de maîtrise en Océanographie

en vue de l'obtention du grade de Maître

PAR

© Robin Accot

Décembre 2015

Composition du jury :

Louis-PhilippeNadeau, président du jury, Université du Québec à Rimouski

Cédric Chavanne, directeur de recherche, Université du Québec à Rimouski

Dany Dumont, codirecteur de recherche, Université du Québec à Rimouski

Suzanne Roy, codirectrice de recherche, Université du Québec à Rimouski

Daniel Bourgault, codirecteur de recherche, Université du Québec à Rimouski

Gustavo Ferreyra, codirecteur de recherche, Université du Québec à Rimouski

Diane Lavoie, examinateur externe, Institut Maurice-Lamontagne

Dépôt initial le 16 décembre 2015 Dépôt final le 8 août 2016

REMERCIEMENTS

Tout d'abord, je souhaite adresser un grand merci à tous mes directeurs : Cédric, Suzanne, Dany, Daniel et Gustavo pour leur confiance et leur soutien dans ce long, voir très long périple qu'a été ma maîtrise.
Une mention Exceptionnelle pour un directeur exceptionnel, Cédric. Tu es une personne profondément gentille et serviable. Grâce à ta pédagogie, à ta disponibilité et à ton dévouement, faire de la recherche à tes côtés ne peut être que pur plaisir.
Dany, merci encore pour tes réponses à mes 1001 questions. De plus, ta bonne humeur permanente, ton ouverture d'esprit et ton sens de l'écoute font de toi une personne très attirante avec qui on aimerait discuter et boire une bière tous les soirs !
Suzanne, Daniel et Gustavo, merci pour le temps que vous m'avez consacré et pour votre aide ô combien précieuse.
Merci à John Ryan, qui m'a accueilli et supervisé durant mon stage à Monterey Bay. Grâce à lui, ma maîtrise a pris une tout autre direction en me permettant d'utiliser des données issues de leurs campagnes ! Encore une personne formidable avec un grand cœur !
Vient maintenant la place de Fred Cyr, qui m'a pris sous son aile à mon arrivée dans le labo de physique. Merci beaucoup pour ton aide, tes réflexions et tout le traitement de données que tu as réalisés pour moi. Merci aussi pour la patience dont tu as fait preuve pour m'initier à matlab !
Mention spéciale pour Laure de Montety, une sublime femme dans tous les sens du terme à qui je souhaite dire un grand merci du fond du cœur.
Merci à James Caveen, Mr informatique, et à Pacal Guillot pour leur aide concernant Linux et le jeu de donnée du SGDO. Rachel, toujours très dynamique et pleine d'initiative concernant les organisations festives ! Martine, secrétaire d'exception qui sait simplifier et aider quiconque fait appel à elle.
Parlons peu, parlons bien ! Wesh Wesh la famille sans qui cette expérience de vie n'aurait pas du tout était la même : Mes collocs : Maman poule (Gwen), Lotus, Aurore et Jeff qui m'ont supporté au quotidien et avec qui j'ai passé de superbes moments. Jennifer Martin, merci, tu m'as fait rêver et apporter beaucoup de joie ! Julien et Mélany, les Québécois par excellence, deux personnes absolument extraordinaires. Filou et Houcem, la mafia au sens littéral, pull up ! Yann, Noémie, Nico, Gab, Quentin, Angy, Mel, Sophia, Kévin, Bizmoot, Mathieu, Mélo, Géraldine, Anne-claire, Barret, Jerem, Yannick, Alex, Enrique, Gauthier, Hamza et Chakib, merci à vous tous d'avoir été là !
Un grand merci à mon équipe de canot à glace, qui m'a fait vivre des expériences hors du commun : Alex, Max, Jo, David.
Un clin d'œil à Hélène qui m'a encouragé à finir mon mémoire. Sans oublier Flo.
Et pour finir merci à ma famille qui malgré tout ce temps ma soutenues, même si des fois ils n'y croyaient plus... Mon père, ma mère et Franck pour son aide dans la dernière ligne droite qu'a été la rédaction.

RÉSUMÉ

L'objectif central de cette recherche était de caractériser les mécanismes physiques, biologiques et chimiques qui affectent les couches minces phytoplanctoniques. Deux environnements marins côtiers différents ont été comparés. Le premier, la Baie de Monterey, est une baie semi ouverte située sur la côte ouest de la Californie. Le deuxième, le Golfe et l'Estuaire Maritime du Saint-Laurent (EMSL), est un système situé sur la côte est du Canada. Contrairement à la Baie de Monterey les couches minces n'avaient encore jamais été étudiées dans le Saint-Laurent et cette étude représente donc une première étape dans ce sens. Des données à haute résolution issues d'un véhicule autonome sous-marin et d'un véhicule sous-marin ondulant ont été utilisées respectivement dans la Baie de Monterey et dans l'EMSL. Les résultats diffèrent selon les régions. Dans l'EMSL les mécanismes affectant les couches minces étaient le cisaillement vertical et le processus d'intrusion de masses d'eau. Les valeurs maximales de cisaillement vertical étaient trouvées au centre des couches minces. De plus, de faibles valeurs du taux de dissipation d'énergie cinétique turbulente ont aussi été mesurées à l'intérieur de ces dernières. Ainsi la stabilité ($Ri > 0.25$) et le faible mélange apparaissent comme des conditions essentielles à l'observation de couches minces. 70 et 77 % des couches minces étaient localisées à l'intérieur de la pycnocline dans l'EMSL et dans la Baie de Monterey respectivement. Dans la Baie de Monterey, la majorité des couches minces étaient localisées dans la nitracline qui se confondait généralement avec la pycnocline. Grâce à des données modélisées il a été montré que le vent pouvait influencer couche de mélange de surface.

Mots clés : Couches minces phytoplanctoniques ; Stratification ; Cisaillement vertical ; Nitracline ; Diffusion turbulente ; Vent

ABSTRACT

The main goal of this research was to characterize the physical, biological and chemical mechanisms that have an effect on the phytoplankton thin layers. Two contrasting coastal marine environments were compared. The first one, Monterey Bay, is a semi-open embayment located on the west coast of California. The second one, the Lower St. Lawrence Estuary (LSLE) and Gulf, is a system located on the eastern coast of Canada. Contrary to Monterey Bay, this work represents the first study of thin layers in the St. Lawrence. High-resolution data obtained from an autonomous underwater vehicle and an undulating underwater vehicle, were used in Monterey Bay and LSLE, respectively. Thin layers were affected by different mechanisms in both regions. In the LSLE, the vertical shear and intrusion processes acted on thin layers. Maximum shear values were found at the center of thin layers. Moreover, low values of dissipation rate of the turbulent kinetic energy were also measured inside thin layers. The stability ($Ri > 0.25$) and the low turbulence appear to be essential conditions to observe thin layers. 70 and 77 % of thin layers were located inside the pycnocline in the LSLE and Monterey Bay respectively. In Monterey Bay the majority of thin layers were located in the nitracline which generally merged with the pycnocline. Through modeled data it was shown that the wind could affect the surface mixing layer.

Keywords: Thin phytoplankton layers; Shear; Stratification; Nitracline; Turbulent diffusion; Wind stress

TABLE DES MATIÈRES

LISTE DES TABLEAUX

LISTE DES FIGURES

INTRODUCTION GÉNÉRALE

Mise en contexte et problématique

Les organismes phytoplanctoniques représentent la base du réseau trophique de nos océans. Grâce à la photosynthèse, ces organismes sont responsables de la production primaire qui est essentielle à la survie des organismes de niveaux trophiques supérieurs. De plus, le phytoplancton est impliqué dans plusieurs cycles biogéochimiques. En effet, les micro-algues marines sont responsables de la fixation annuelle de 40 % du carbone fixé par la totalité de la biosphère (Falkowski 1994). Leur étude et la compréhension des mécanismes qui gouvernent leur développement sont donc essentielles.

Le milieu pélagique est un environnement en continuel mouvement où règne une hétérogénéité spatiale. Cette hétérogénéité se reflète dans la distribution du phytoplancton. Comme mentionné dans de nombreuses études, ce dernier possède un caractère agrégatif et se retrouve généralement sous forme de « patch » phytoplanctonique dans la colonne d'eau (Bainbridge 1957; Haury et al. 1978; Levasseur et al. 1983). Dépendamment de l'échelle spatiale à laquelle on se situe pour l'étudier, différents facteurs peuvent être la cause de cette hétérogénéité. Tel que proposé par Haury et al. (1978), les échelles spatio-temporelles des patrons et des processus liés au phytoplancton sont classées selon les méga-, macro-, méso-, grossière-, fine-, et micro-échelles.

Dans la présente étude, nous nous intéressons à l'échelle grossière (1 à 100 km) et à l'échelle fine (1 m à 1 km). Dans ces ordres de grandeur les mécanismes frontaux, les résurgences (upwellings), les interactions inter- et intra-espèces et les concentrations en nutriments sont les facteurs clés de contrôle du développement des algues phytoplanctoniques. Avec l'apparition de sondes et d'instruments plus performants pour l'échantillonnage à fine échelle, une structure bien particulière du phytoplancton a été mise à jour, les couches minces. Pour être nommée ainsi cette structure doit répondre à trois critères issus d'un consensus et définis par Dekshenieks et al. (2001) et Sullivan et al. (2010). Il s'agit de l'agrégation du phytoplancton sur une faible épaisseur verticale (1),

inférieure à 3 m, avec une concentration qui est au moins deux fois supérieure à celle alentour (2). De plus, cette structure doit être temporellement persistante, c'est-à-dire visible sur plusieurs profils verticaux successifs (3). Le critère de persistance est un moyen supplémentaire pour vérifier que cette structure n'est pas due à un artefact de mesure. Ainsi, concernant la persistance temporelle il n'existe pas réellement de durée et de nombre de profils minimums. Les couches minces peuvent être assimilées au maximum de chlorophylle de sous surface ou à toute autre structure existante, du moment que cette dernière répond aux 3 critères précédemment énoncés.

Les couches minces font l'objet d'études intensives depuis plus de 10 ans, et la première d'entre elles a été observée en 1968 (Strickland 1968). Leur importance est due au fait qu'elles peuvent atteindre jusqu'à 55 fois les valeurs de fluorescence/chlorophylle a à leur base (Ryan et al. 2008) et représenter plus de 50 % de la biomasse totale de chlorophylle avec une fréquence d'occurrence dans les profils verticaux pouvant atteindre 87 % (Sullivan et al. 2010). Elles ont déjà été observées dans des baies (Ryan et al. 2008), des Golfes (Steinbuck et al. 2010), des Estuaires (Kasai et al. 2010), des fjords (Dekshenieks et al. 2001), des lacs (Yamazaki et al. 2010) et dans l'océan (Churnside and Donaghay 2009). Elles peuvent s'étendre sur des distances horizontales supérieures à 20 km (Johnston et al. 2009) et contenir des espèces phytoplanctoniques toxiques (Rines et al. 2002; McManus et al. 2008; Sullivan et al. 2010).

Six mécanismes principaux peuvent être responsables de la formation des couches minces phytoplanctoniques (Figure 1, tirée de Durham and Stocker 2012). Plus de la moitié des mécanismes résultent de l'interaction entre des phénomènes biologiques et physiques de la colonne d'eau (Figure 1b, c, d, e). Les autres mécanismes sont une conséquence directe qu'exerce le milieu physique sur le phytoplancton et ne dépendent donc pas de critères biologiques (Figure 1a, f). Parmi ces derniers, on note 1) l'influence que peut avoir un cisaillement vertical sur un patch phytoplanctonique (Figure 1a) ou bien 2) l'intrusion d'une masse d'eau dans un patch de phytoplancton (Figure 1f). Dans les deux cas le patch sera étiré horizontalement pour une période plus ou moins longue.

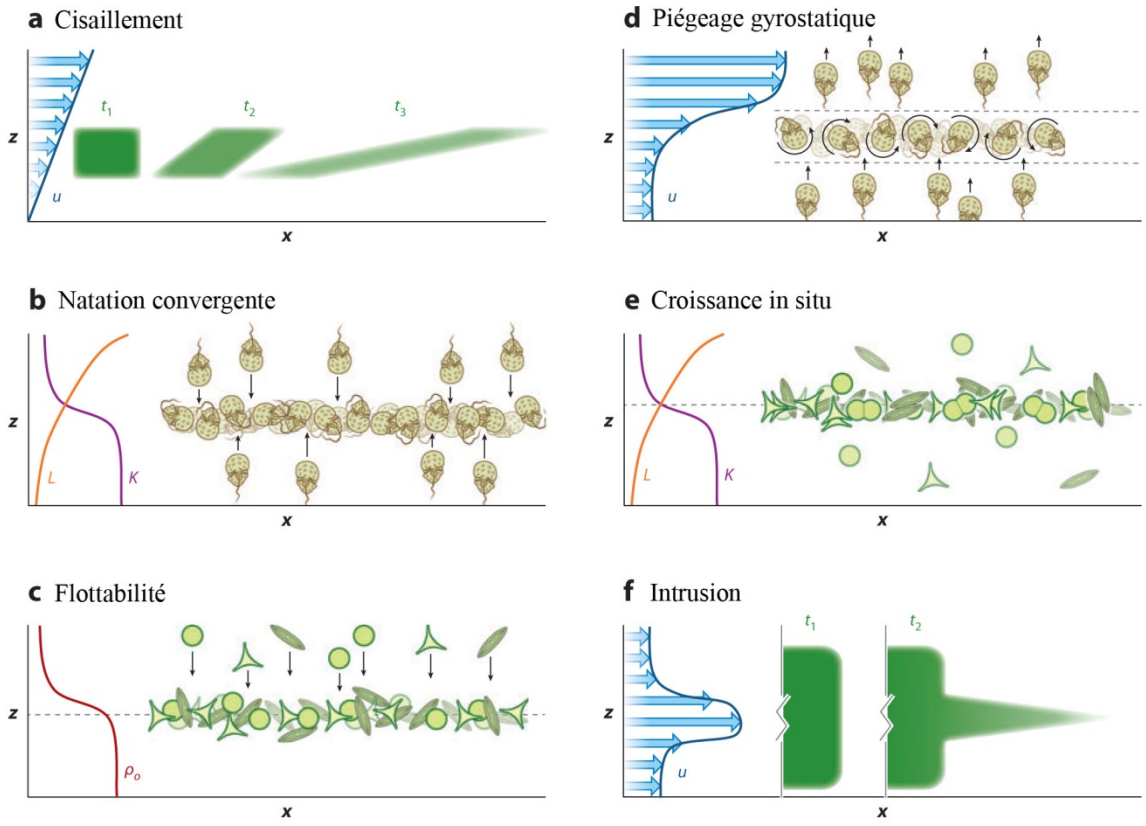

Figure 1 Mécanismes de formation des couches minces phytoplanctoniques (modifié de Durham and Stocker, 2012). L, K et ρ_0 correspondent respectivement aux courbes d'intensité lumineuse, de nutriments et de densité.

Néanmoins pour former une couche mince, il faut que l'étendue du patch initial soit plus petite que le déplacement induit par le mécanisme de cisaillement ou d'intrusion. Il peut aussi se produire ce qui est communément appelé 3) un « piégeage gyrostatique » (Figure 1d). C'est le cas lorsqu'une cellule mobile de phytoplancton migre et se retrouve dans un fort cisaillement vertical. Si ce cisaillement possède une intensité supérieure au seuil permettant à la cellule d'être maître de son déplacement, alors cette dernière se retrouvera piégée dans cette zone, où il y aura accumulation. Les trois derniers mécanismes concernent le développement du phytoplancton lorsque celui-ci se trouve dans une zone avec une intensité lumineuse et une quantité de nutriments suffisants à sa croissance. Des couches minces peuvent ainsi se former (4) lorsque des espèces phytoplanctoniques non mobiles sont initialement présentes dans une telle zone (Figure 1e). (5) De plus, certaines

espèces non-mobiles telles que *Trichodesmium spp.* sont aussi capable de modifier leur densité jusqu'à atteindre une profondeur de densité neutre pour réaliser des migration verticales, Figure 1c (White et al. 2006). (6) Pour finir, la motilité de certaines espèces phytoplanctoniques, tel qu'*Akashiwo sanguinea*, peut leur permettre d'atteindre directement une zone favorable à leur développement, Figure 1b (Sullivan et al. 2010).

Les couches minces phytoplanctoniques, notamment celles contenant des algues toxiques, peuvent avoir des répercussions néfastes sur l'écosystème. La Baie de Monterey est souvent soumise à des floraisons d'algues toxiques. Ainsi, suite à une floraison de *Akashiwo sanguinea*, une mortalité massive d'oiseaux de mer a été observée (Jessup et al. 2009). De plus, la présence de toxines à l'intérieur de poissons et de crustacés a déjà été répertoriée (Jester et al. 2009). L'impact économique des algues toxiques aux États-Unis est estimé entre 33 et 82 millions de dollars par an (McManus et al. 2008). Dans le but de pouvoir prédire le développement des couches minces, un grand nombre d'études a été réalisé dans la Baie de Monterey. Celles-ci visaient à comprendre quels étaient les mécanismes qui contribuent à leur formation et à leur dynamique (McManus et al. 2003, 2008; Ryan et al. 2008, 2009, 2010; Steinbuck et al. 2009; Rines et al. 2010; Moline et al. 2010; Sullivan et al. 2010). Cette liste non exhaustive d'études met en valeur la difficulté de réunir toutes les observations nécessaires dans le temps et dans l'espace pour confirmer et déterminer avec certitude quels mécanismes sont responsables de la formation des couches minces.

C'est dans le cadre de cette problématique générale qu'une investigation a été réalisée dans le Saint-Laurent où l'étude des couches minces n'a encore jamais été réalisée jusqu'à l'heure actuelle. De plus, une comparaison a été effectuée avec les couches minces répertoriées lors d'une mission en mer dans la Baie de Monterey.

Objectifs

L'objectif de cette étude est de caractériser :

1) La distribution des couches minces, leurs similarités et leur différences à l'intérieur de deux régions différentes : le Saint-Laurent et la Baie de Monterey.

2) Les différents processus physiques, biologiques et chimiques agissant sur les couches minces de l'estuaire maritime du Saint-Laurent et de la Baie de Monterey.

Méthodologie

Pour répondre au premier objectif, trois jeux de données ont été utilisés afin de caractériser au mieux l'échelle spatiale dans le Saint-Laurent. Ainsi, 13720 profils de fluorescence répartis dans tout le Golfe et l'Estuaire ont été analysés dans le but de détecter la présence de couches minces (Figure 3). Parmi ces profils, le premier jeu de donnée (1) correspond à 10992 profils CTD. Ces derniers ont été réalisés par le Ministère Pêche et Océan et obtenu par l'Observatoire Global du Saint-Laurent (OGSL) qui permet d'interroger le système de gestion des données environnementales et d'obtenir les données archivées à l'Institut des Sciences de la Mer à Rimouski et à l'Institut Maurice-Lamontagne. Ces derniers ont été réalisés entre 1999 et 2014 et étaient répartis dans tout le Golfe et l'Estuaire. De plus, 1772 profils provenaient de différentes missions effectuées le long d'un axe transversal en face de Rimouski et à Tadoussac entre 2009 et 2012 durant l'été, (2). Pour finir, du 15 au 18 mai 2013, une mission s'est déroulée dans l'EMSL et a fourni les derniers 956 profils, (3). Les données de l'OGSL ont été utilisées dans le seul but de détecter la présence des couches minces et leurs caractéristiques. Seules les autres données ont servi à comparer les couches minces avec les autres variables mesurées lors de l'analyse du deuxième objectif. Concernant la Baie de Monterey en Californie, l'échantillonnage fut effectué principalement dans la partie nord-est (Figure 2). Quatre missions réalisées les 13, 14 et 16 août 2013, ainsi que le 19 septembre 2013 ont permis d'obtenir un total de 650 profils.

Afin de caractériser les processus physiques, biologiques et chimiques, différentes variables ont été mesurées dépendamment des régions. Celles-ci sont résumées dans le Tableau 1.

De plus des données de températures de surface, de vent et d'élévation du niveau de la mer mesurées à partir de satellite et de station météorologique étaient également disponibles.

Les principaux résultats de cette étude sont présentés ci-après sous la forme d'un manuscrit à soumettre pour publication dans une revue scientifique à comité de lecture.

Tableau 1 Variables mesurées dans chaque région

Types de variables	Variables \ Régions	Baie de Monterey	Saint-Laurent
Physique	Cisaillement vertical (s^{-1})		X (P)
	Turbulence [1] ($W.kg^{-1}$)		X (P)
	Température (°C)	X (P)	X (P)
	Salinité (PSU)	X (P)	X (P)
	Optique [2] (m^{-1})	X (P)	
Biologique	Fluorescence relative	X (P)	X (P)
	Performance photosynthétique		X (P)
	Taxonomie		X (B)
Chimique	Nitrate (µm)	X (P)	X (P)

[1] correspond au taux de dissipation d'énergie cinétique turbulente
[2] correspond à la rétrodiffusion optique avec les longueurs d'onde 420 nm et 700 nm.
Données issues de profils, P, ou de bouteilles, B.

CHARACTERIZATION OF PHYTOPLANKTON THIN LAYERS AND A COMPARISON OF THE MECHANISMS AFFECTING THEM IN THE LOWER ST. LAWRENCE ESTUARY AND MONTEREY BAY

1.1 INTRODUCTION

Since the first observation of thin phytoplankton layers was reported (Strickland 1968), knowledge about mechanisms that can cause them has increased significantly. These layers have a fine-scale vertical structure (cm to a few meters) but a relatively large horizontal extent up to tens of kilometers (Hodges and Fratantoni 2009; Johnston et al. 2009; Ryan et al. 2010). They are biological "hotspots", because they are often associated with layers of zooplankton, bacteria, marine snow, and bioluminescence (McManus et al. 2003). Thin layers have been found to have chlorophyll a concentration up to 55 times greater than the background values (Ryan et al. 2008) and a frequency of occurrence in vertical profiles varying between 0.2% in Alaska near Kodiak Island (Churnside and Donaghay 2009) and 87% in Monterey Bay, California (Sullivan et al. 2010). Also, they may be dominated by one or several species of phytoplankton, including toxic algae, such as *Pseudo-nitzschia australis* and *Akashiwo sanguinea* (McManus et al. 2008; Rines et al. 2010).

While the use of universal criteria to define thin layers is difficult, because it depends on instruments and environmental conditions (Sullivan et al. 2010), it is nonetheless required in order to compare results obtained from different study area and using different methodologies. Three criteria, defined by Dekshenieks et al. (2001) and Sullivan et al. (2010), are commonly used: 1) thin layers must be spatially and temporally persistent; 2) the fluorescence/chlorophyll structure must have a full-width-half-maximum (FWHM) range less than 3 meters; 3) the fluorescence/chlorophyll maximum must be at least twice higher than the background.

Different physical and biological processes can be involved in the formation, maintenance and dissipation of thin layers. The main physical processes are the vertical shear (Birch et al. 2008; Ryan et al. 2008), the turbulent diffusion (Stacey et al. 2007; Wang and Goodman 2010), the intrusion of a water layer (Kasai et al. 2010) and the stratification of the water column (Dekshenieks et al. 2001). Stratification favors the development of thin layers (Ryan et al. 2010; Steinbuck et al. 2010) by limiting the turbulence, such as in the pycnocline where thin layers are often localized (McManus et al. 2008). Although some dinoflagellates have the capacity to tolerate high turbulence levels that typically occur in frontal and coastal upwelling zones (Smayda 2002), turbulent diffusion generally dissipates thin layers. However, frontal zones can generate shear and intrusions of water inside patches of phytoplankton which favor the formation of thin layers (Ryan et al. 2008; Johnston et al. 2009; Kasai et al. 2010). Concerning the biological mechanisms, some phytoplankton cells can modify their buoyancy and/or swim towards nutrient-rich waters (Ryan et al. 2010; Sullivan et al. 2010). To be temporally persistent, mechanisms of convergence must dominate or be in balance with mechanisms of divergence otherwise they will be destroyed.

Signatures of thin layers have been recorded in a wide variety of environments such as bays (Ryan et al. 2008), gulfs (Steinbuck et al. 2010), estuaries (Kasai et al. 2010), fjords (Dekshenieks et al. 2001), lakes (Yamazaki et al. 2010) and open ocean (Churnside and Donaghay 2009). Here, we compare observations from two contrasting places, a bay (Monterey Bay) and an estuary (Lower St. Lawrence Estuary), to investigate whether similar or different physical processes influence the formation of thin layers in different environments.

Monterey Bay is a semi-open embayment located on the west coast of California along the eastern margin of the North Pacific. It is 19 km wide in the east-west direction and 37 km long in the north-south direction, Figure 2 (Graham and Largier 1997).

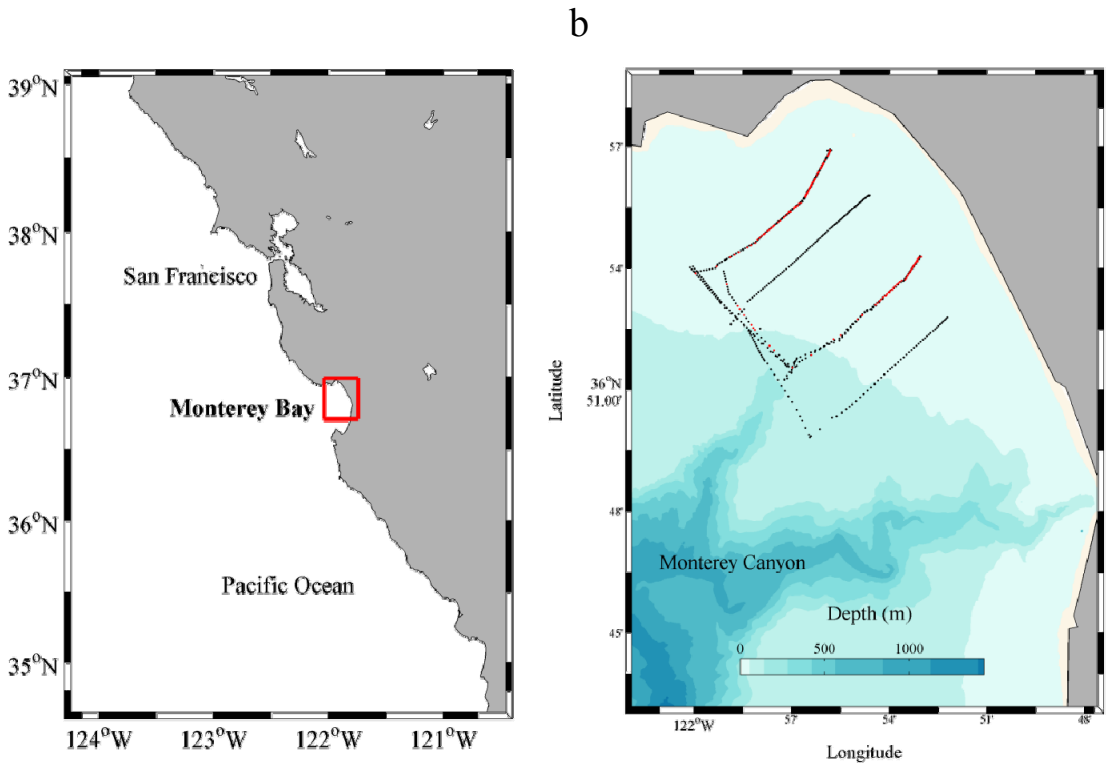

Figure 2 a) Localization and b) bathymetry of Monterey Bay. Black dots are CTD and fluorescence casts and red ones are those containing a thin layer.

In the northern part of the bay there is a cyclonic circulation with a recirculation of warmer waters (Graham and Largier 1997). The Monterey Bay canyon transports nutrients from the deep shelf to the euphotic zone inside the bay that influence phytoplankton productivity (Ryan et al. 2005). Cold and nutrient-rich waters allow for the presence of high chlorophyll a concentrations in the bay (Barber and Smith 1981). The equatorward wind and southward transport of surface water are characteristic of the upwelling period that occurs during spring and summer (Strub et al. 1987; Pennington and Chavez 2000). Two upwelling systems generally develop in the north and in the south of Monterey Bay near Point Año Nuevo and Point Sur, respectively (Rosenfeld et al. 1994). Upwelling plumes and fronts are also common features during active upwelling (Rosenfeld et al. 1994). It is followed by a relaxation period that is called the *oceanic period*, because equatorward winds weaken and California Current water replaces upwelled water (Skogsberg and Phelps 1946).

Phytoplankton blooms weaken before reaching an annual minimum during winter, the *Davidson Current period* (Pennington and Chavez 2000). In 2002 the Coastal Ocean Exploration: Searching for Thin Layers project reported intense thin layers in Monterey Bay, which spurred many research projects (e.g. the Autonomous Ocean Sampling Network, the Layered Organization in the Coastal Ocean) and publications (Rines et al. 2002; McManus et al. 2003; Sullivan et al. 2003, 2010; Ryan et al. 2008, 2009, 2010; Steinbuck et al. 2009; Moline et al. 2010) to understand the physical, biological and chemical processes that contribute to thin layer dynamics.

The Lower St. Lawrence Estuary (LSLE) and the Gulf of St. Lawrence (GSL) constitute a semi-enclosed system, open to the Atlantic Ocean through the Cabot Strait and Strait of Belle Isle, Figure 3. Both are located on the east coast of Canada. The freshwater discharge of the St. Lawrence River and other rivers, coupled to the relatively warm and salty bottom layer, approximately 5°C and 34.8 psu (Gilbert et al. 2005), originating from the Atlantic Ocean, are responsible for the residual estuarine circulation in the LSLE (Koutitonsky and Bugden 1991). The LSLE has a length of 200 km, a mean width of 40 km and is connected to the GSL by a former glacial valley, the Laurentian Channel, which has a maximum depth of 350 m in the estuary. In winter, the water column is stratified in two layers, a cold and fresh surface layer overlying a warmer and saltier deep layer. During summer the upper part of the surface winter layer warms, while the lower part remains cold becoming a cold intermediate layer (Banks 1966). Cyr and Larouche (2015) observed the presence of many quasi-permanent fronts in the Gulf and in the LSLE. In this region, the formation mechanisms of fronts are the result of the combination of many factors: the tidal mixing, the upwellings due to the dominant wind, the cross-estuary current and gyres (Cyr and Larouche 2015). Nutrients are generally not limiting in the photic layer so growth of phytoplankton depends on the stability of the water column and light (Vandevelde et al. 1987). The LSLE is characterized by an important phytoplankton bloom during summer and a second one, generally weaker, in fall (Levasseur et al. 1984).

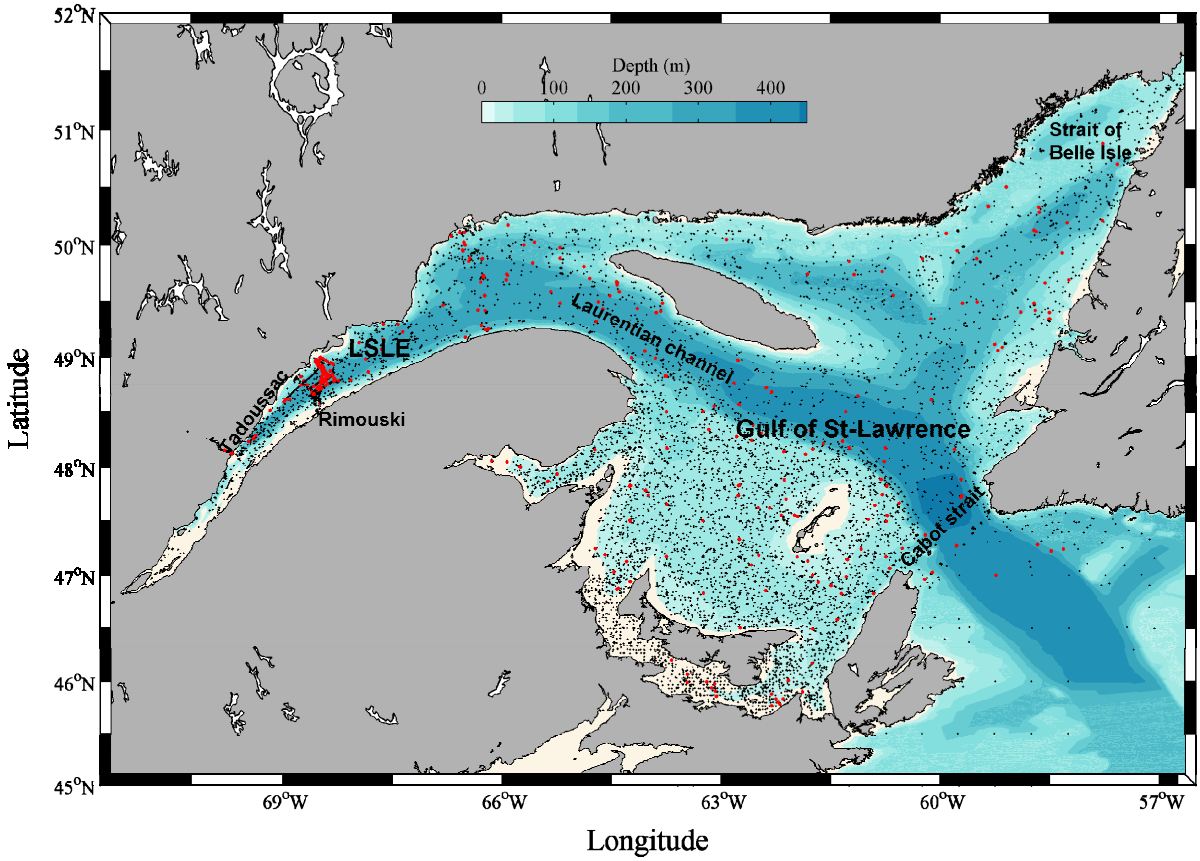

Figure 3 Map of the Gulf of St. Lawrence and the Lower St. Lawrence Estuary. Black dots are CTD and fluorescence casts and red ones are those containing a thin layer.

Furthermore, diatoms with a size larger than 20 µm, like *Thalassiosira nordenskioeldii*, *Chaetoceros debilis* and *Nitzshia seriata* represent the dominant fraction of phytoplankton biomass during summer (Levasseur et al. 1984; Roy et al. 1996). The LSLE width (40 km), which is several times the internal Rossby radius (~ 10 km), promotes the development of mesoscale (>10 km) and sub-mesoscale (<10 km) flow structures, such as fronts and eddies (Ingram and El-Sabh 1990; Mertz and Gratton 1990; Cyr and Larouche 2015). Dynamic stability of the water column (determined by the Richardson number), stratification, turbidity, internal waves, vertical shear rate, advection, nutrient concentration and irradiance in the water column are factors that are modulated by the dynamics of fronts

(Vézina et al. 1995; Savenkoff et al. 1997), impacting on the distribution and productivity of phytoplankton (Demers and Legendre 1981; Vandevelde et al. 1987; Levasseur et al. 1992). Despite their importance for the marine environment, no comprehensive study on thin layers has ever been published for the St. Lawrence to our knowledge.

The aim of the present work (1) is to characterize the spatial and temporal distribution of thin layers and their similarities and differences in two distinct and contrasting sites: the St. Lawrence and Monterey Bay; and to investigate (2) the physical, biological and chemical processes acting on LSLE and Monterey Bay thin layers.

1.2 MATERIALS AND METHODS

1.2.1 Sampling

St. Lawrence. A mission was undertaken from 15 to 18 May 2013 in the LSLE on board the *R/V Coriolis II*. Thereafter we will call it the LSLE mission. Eight transects were done using an undulating underwater vehicle, the EIVA Scanfish II (SF) and six stations were sampled. The SF was towed behind the ship with a horizontal speed of 3.8 m s^{-1} and a vertical speed of 0.76 m s^{-1}. Using the SF a total of 952 vertical profiles were acquired between ~2 m depth and a maximum of 100 m depth for a total distance of 341 km. The horizontal resolution between two profiles was ~0.37 km. It was equipped with a CTD (Conductivity, Temperature, Depth) Seabird SBE-49 (16 Hz), and a WetLabs ECO Fluorometer and turbidity sensor (1 Hz). During the stations a system comprising a Seabird Carousel SBE-32 with 12x12L-bottles, a CTD Seabird SBE-911 plus, a SBE-43 Dissolved Oxygen, a WetLabs ECO Fluorometer, a WetLabs transmissometer, a Campbell Scientific OBS-3+ turbidity sensor, and an *in situ* ultraviolet spectrophotometer (ISUS-V3) nitrate sensor profiled the entire water column. The ratio of variable fluorescence (the difference between the maximum and minimum fluorescence yield measured in dark-adapted phytoplankton) to maximum fluorescence (F_v/F_mratio, an estimate of the photochemical quantum yield of photosystem II), was used to assess the photosynthetic performance. F_v/F_m measurements were performed with a Fast Repetition Rate fluorometer (FRRf, Chelsea Technologies, UK). Water samples were analyzed with an optical microscope to determine the dominant phytoplankton genera. The *R/V Coriolis II* was equipped with an Acoustic Doppler Current Profiler (RDI 150 kHz Ocean surveyor), and current profiles were measured with a vertical resolution of 4 meters. Some technical problems caused the temporary shutdown of the ADCP for some transects. Wind data from Maurice Lamontagne Institute buoy, IML-4 (48.66°N, 68.58°W) were downloaded from the St. Lawrence Global Observatory-SLGO, (http://slgo.ca, 2014) with a 15-minute temporal resolution. Hourly water level was obtained from the Rimouski station #2985 by Fisheries

and Oceans Canada. During the study period we also used sea surface temperature (SST) from the Moderate Resolution Imaging Spectroradiometer (MODIS) with 1 km spatial resolution (http://oceancolor.gsfc.nasa.gov/cms/).

The second LSLE dataset consists of 291 casts from 7 missions undertaken between July and October 2009, 750 casts from 25 missions between May and October 2010, 635 casts from 17 missions between May and November 2011 and 72 casts from one mission in October 2012. A fixed station was done in 2010 at 48.47 °N latitude and 68.50 °W longitude, and 24 casts were realized in less than 3 hours. Among the 1772 casts, 1555 were located along a transverse axis in front of Rimouski and 217 casts were performed near Tadoussac (Figure 3). Thereafter these will be called the transverse axis missions. All the profiles of these missions were sampled by Cyr et al. (2011, 2015). Most missions were conducted opportunistically, depending on boat availability and the weather. A vertical microstructure profiler (VMP) manufactured by Rockland Scientific International (RSI) was used. The VMP was equipped with a SBE CTD, a microfluorescence/turbidity sensor, two Thermometrics fast-response thermistors, and two airfoil shear probes. The sampling rate for the CTD sensor was 64 Hz and 512 Hz for the other sensors. Details of all the equipment are given in Bourgault et al. (2008) and Cyr et al. (2011, 2015).

The last dataset consists of 10992 casts from 178 missions undertaken from 1999 to 2014 by Fisheries and Oceans Canada that were downloaded from SLGO (2014). Data cover the period from March to November and are distributed in the entire GSL and LSLE (Figure 3). This dataset will be called the historical missions. Depending on the missions, different fluorescence sensors were used. Fluorescence was therefore used as a proxy for phytoplankton concentration to investigate the presence of thin layers in profiles.

Monterey Bay. An Autonomous Underwater Vehicle (AUV), Dorado, from Monterey Bay Aquarium Research Institute performed a high resolution mapping of eight transects and 622 profiles in the north of the Bay (Figure 2b). The same area was sampled on 13, 14, 16 August and 19 September 2013. Two transects were performed each day.

The AUV track was ~ 86 km long with a speed of ~1.16 m s^{-1} which represents a horizontal resolution between profiles of ~ 0.26 km. The chlorophyll fluorescence, optical backscattering (420 and 700 nm) and nitrate values were measured by a HOBI Labs HS-2 sensor and an ISUS, respectively (Johnson and Coletti 2002). The AUV was also equipped with a SeaBird SBE 25 CTD sensor. Wind was measured at Long Marine Lab (LML, 36.95°N, 122.07°W) with an hourly temporal resolution and sea level was measured at the station 9413450 (36.60°N, 121.88°W). We also used daily-averaged sea surface temperature from the Group for High Resolution Sea Surface Temperature (GHRSST) with 1 km spatial resolution (http://ourocean.jpl.nasa.gov/SST/).

1.2.2 Data processing

1.2.3.1. Sensors

A mobile median filter of three points was applied for every sensors of the AUV to reduce noise spikes. All physical measurements for the transverse axis missions were processed by Cyr et al. (2011, 2015). Thereafter, all variables were averaged every 10 cm except for the fluorescence of the LSLE missions which has a lower resolution.

Water samples were not taken during transects for all missions in the LSLE and Monterey Bay, so there were no discrete chlorophyll measurements and it was thus not possible to convert fluorescence to chlorophyll concentration. In order to compare data sets together, it was decided to use relative fluorescence. For the LSLE mission, the time corresponding to the measurements of fluorescence was not recorded by the fluorometer. In this way fluorescence was manually manipulated in each transect to fit with the time data of the CTD. The manipulations were performed with a subjective interpretation of the data to ensure the consistency of fluorescence profiles. Fluorescence and CTD time series were adjusted so that subsurface fluorescence maxima occurred at the same depth on consecutive up and down casts. The vertical resolution of the current measurements was 4 m, and we used a moving average of 30 minutes to reduce noise for the LSLE mission.

Therefore the vertical shear and the Richardson number have also a vertical resolution of 4 m. The nitrate sensor baseline reference can vary from survey to survey, because the nitrate sensor was not calibrated.

In Monterey Bay, the nitrate data was used to determine the location of the nitracline in order to characterize the environment of phytoplankton thin layers.

1.2.3.2. Method used to define thin layers and their characteristics

Thin layers of fluorescence were determined using the three criteria defined by Dekshenieks et al. (2001) and Sullivan et al. (2010) except for the historical missions. (1) Thin layers must be spatially and temporally persistent; (2) the fluorescence/chlorophyll structure must have a FWHM range less than 3 meters; (3) the fluorescence/chlorophyll maximum must be at least twice higher than the background. To measure the intensity of a thin layer (or height of the fluorescence maximum, criterion 3), the fluorescence background was calculated by linearly interpolating fluorescence between the top and bottom of a thin layer structure. Then the fluorescence maximum was divided by his interpolated value. Moreover, to calculate the thin layer's normalized fluorescence we have calculated the ratio between the relative fluorescence divided by the maximum relative fluorescence of the thin layer multiplied by the fluorescence maximum intensity ratio of thin layer. In the historical mission, it was not possible to verify the temporal persistence, criterion (1), because there were no time series. As in others studies (Dekshenieks et al. 2001), to ensure that thin layers were not due to measurement errors, we verified that a minimum of six data points of fluorescence were obtained inside the layer. For some analyses in the LSLE and Monterey Bay, thin layers were compared to non-thin layers structure. Each fluorescence layer which did not respect one of the three criteria was considered as a non-thin layer.

The thin layers occurrence frequency in profiles, was calculated as the number of profiles that contained a thin layer divided by the total number of profiles.

1.3 RESULTS

1.3.1 Thin layers characteristics

Thin layers were observed during the Monterey Bay missions (Figure 2) and in the St. Lawrence Gulf and Estuary, where the first one was observed in 2001 (Figure 3). The occurrence of thin layers was smaller in the St. Lawrence, from 1% to 14% with a mean of 3 %, compared to Monterey Bay, 24% (Table 2).

Between the St. Lawrence's datasets, the highest occurrence was observed during the LSLE mission, 14 %, which focused on frontal regions. In addition, inside the Gulf and the Estuary of the St. Lawrence thin layers occurrence varied temporally, although sampling did not allow to properly resolve seasonal variability (Figure 4). The majority of profiles were done from May to August. The thin layer's occurrence was more important in May, June and August compared to other periods (Figure 4). During the Transverse axis missions in August, only 47 profiles were realized and all profiles with thin layers profiles (19) were found during the same mission, which explains the high occurrence for this dataset. Moreover, the thin layer's FWHM was in the same order of magnitude in the different datasets of the St. Lawrence while their intensity was stronger in the Historical missions than others (Table 2). Furthermore, in the St. Lawrence the thin layer's depth varied widely (Table 2, Figure 5). They were generally present between the surface and 25 m depth and some were observed up to 70 m depth in the LSLE and Historical missions (Figure 5Figure 6). In the LSLE, the thin layer and non-thin layer relative fluorescence profiles followed generally the same trend with a relative fluorescence concentrations significantly different (Figure 6). The relative fluorescence had a maximum concentration near the surface between 0 and 20 m before decreasing in depth where another local maximum was located between 50 and 70 m.

Table 2 Characteristics of thin layers in all datasets.

	St. Lawrence			Monterey Bay
	Historical missions	Transverse axis	LSLE	
Number of profiles	10992	1772	956	650
Occurence of thin layers in profiles (%)	3	1	14	24
FWHM[1] (m)	1.8	1.4	2.2	1.8
Intensity (ratio)	4.8	2.3	2.8	3.2
Depth (m)	20	12	16	8

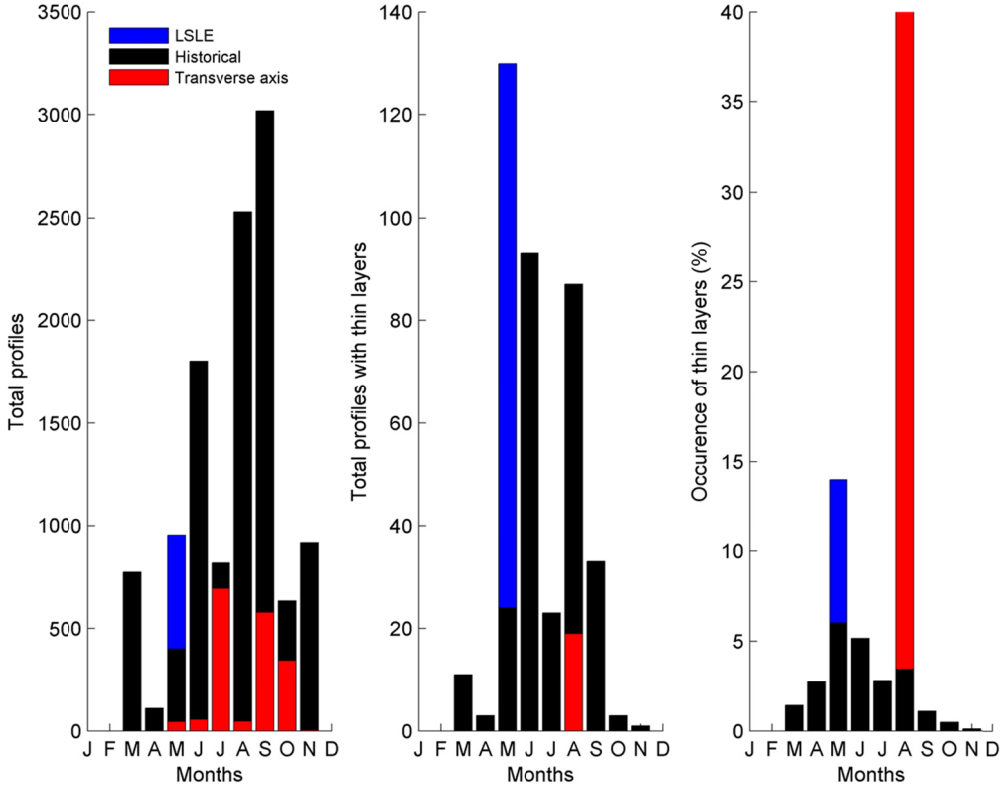

Figure 4 Sampling in the St. Lawrence showing the profiles and thin layers per month for all datasets

At four fixed stations in the LSLE, (17, 18 May 2013) water samples were analyzed at different depths (2m, 5m, 45m and 100m). Phytoplankton abundance was dominated by diatoms (*Thalassiosira nordenskioeldii* and *Skeletonema costatum*). In this region, thin layers extended on a horizontal distance up to 12 km (not shown).

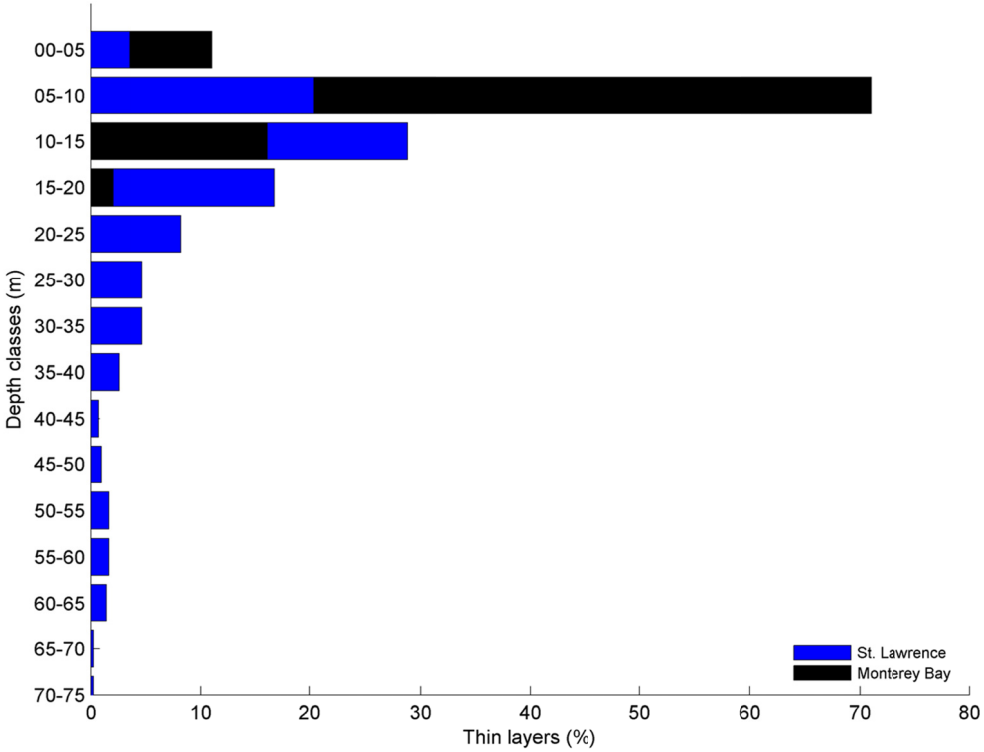

Figure 5 Thin layer's vertical location in both regions

In Monterey Bay, thin layers were observed during all missions except on 19 September 2013, and they were mainly located near the coast (Figure 2b). In this region, thin layers extended on a horizontal distance up to 8 km (16 August 2013 transect). They corresponded most of the time to the subsurface fluorescence maximum (SFM) around 8 m depth (Figure 5 andFigure 6). Moreover, thin layer's relative fluorescence was higher than the concentration inside non-thin layers (Figure 6).

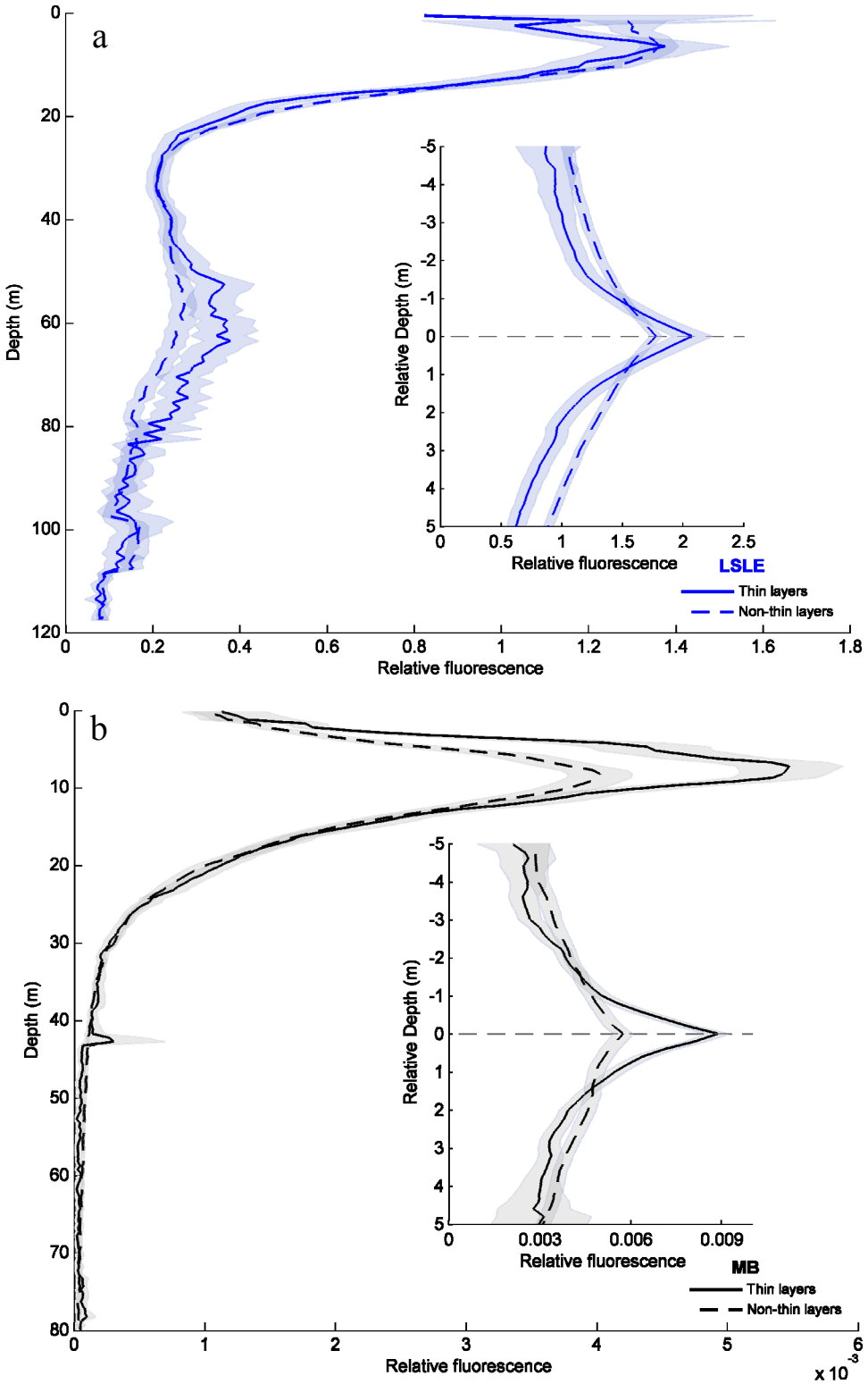

Figure 6 Mean profile of relative fluorescence for thin layers and non-thin layers in a) the Lower St. Lawrence Estuary (dataset: LSLE) and b) Monterey Bay. In the insets, depth is relative to the center of thin layers, with negative values above and positive values below. Only the relative fluorescence profiles inside thin and non-thin layers are used for the inset.

Their intensity, 3.2, and their FWHM, 1.8 m, were in the same order of magnitude than thin layers inside the St. Lawrence (Table 2, Figure 7). However, using two characteristics it was possible to differentiate both regions. First, the ratio of relative fluorescence in thin layers to that in non-thin layers was stronger in Monterey Bay than in LSLE (Figure 6). Second, thin layers were deeper in the St. Lawrence compared to Monterey Bay. This depth difference could be mostly explained by the physical and chemical conditions and the dynamics of the water column, as shown below.

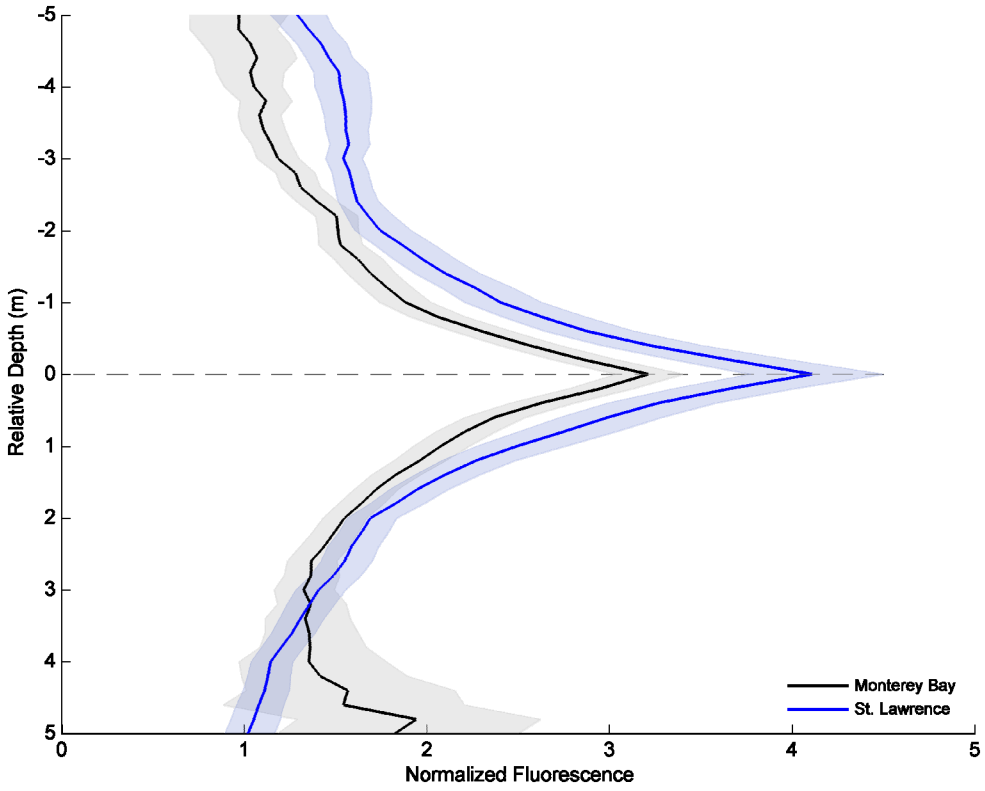

Figure 7 Thin layer's normalized fluorescence in both regions

1.3.2 Physical conditions inside thin layers

The water density is mainly controlled by salinity in the LSLE and by temperature in Monterey Bay. The stratification of the water column is quantified with buoyancy frequency (s^{-1}) which was calculated as:

$$N = \sqrt{-\frac{g}{\rho_w}\frac{\partial \overline{\sigma_t}}{\partial z}}, \qquad (1)$$

where g = 9.81 m s^{-2} is the gravitational acceleration, ρ_w = 1052 kg m^{-3} is a reference density, $\overline{\sigma_t}$ represents the density data that have been smoothed using a mobile mean of 50 cm, and z the upward axis. The buoyancy frequency was greater in the LSLE than in Monterey Bay, respectively $5.08\times10^{-2}\,s^{-1}$ and $3.55\times10^{-2}\,s^{-1}$ (Figure 8). Maxima of stratification were located above the center of thin layers in Monterey Bay and below the center in the LSLE (Figure 8). Thin phytoplankton layers were mostly located at the nitracline depth, which often coincided with the pycnocline, except in a few places.

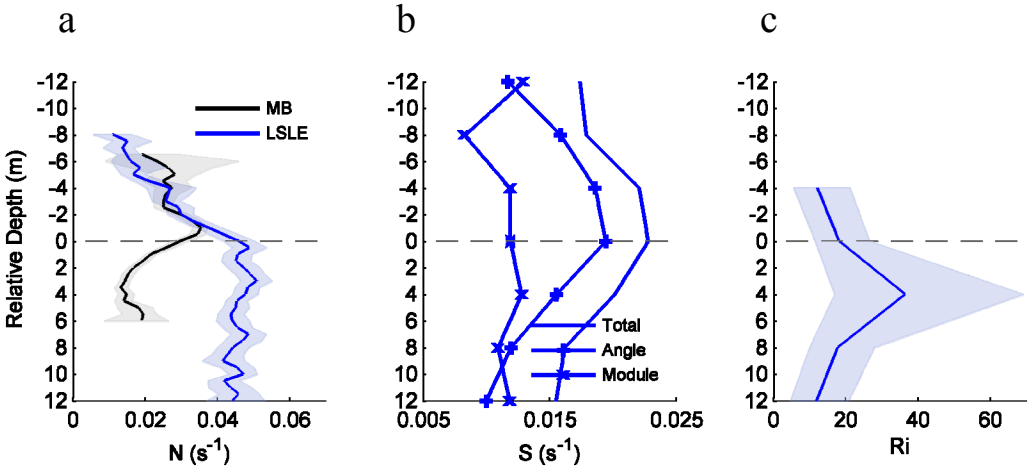

Figure 8 Mean profiles for thin layers of a) buoyancy frequency, b) vertical shear and c) the Richardson number. In a) and c) shadings represent the 95% confidence intervals. Depth is relative to the center of thin layers, with negative values above and positive values below. Only the buoyancy frequency was calculated for Monterey Bay.

The weaker density stratification in Monterey Bay probably allows phytoplankton to sink below the pycnocline where the nitracline is found in a few places (Figure 9).

The Richardson number (Ri) was calculated as:

$$Ri = N^2 / S^2 , \tag{2}$$

where vertical shear, S (s^{-1}), is given by :

$$S = \sqrt{\left(\frac{\partial u}{\partial z}\right)^2 + \left(\frac{\partial v}{\partial z}\right)^2} . \tag{3}$$

To calculate Ri , values of the buoyancy frequency have had average 2 m at the top and bottom of the vertical shear depth for each depth. Inside thin layers, Ri was greater than 0.25 indicating stable conditions for Kelvin-Helmholtz instabilities (Figure 8). Maximum values of Ri (36.4) were located below the center of thin layers due to the strong stratification in the pycnocline. Figure 10 shows, in more details, the location of thin layers relative to the pycnocline.

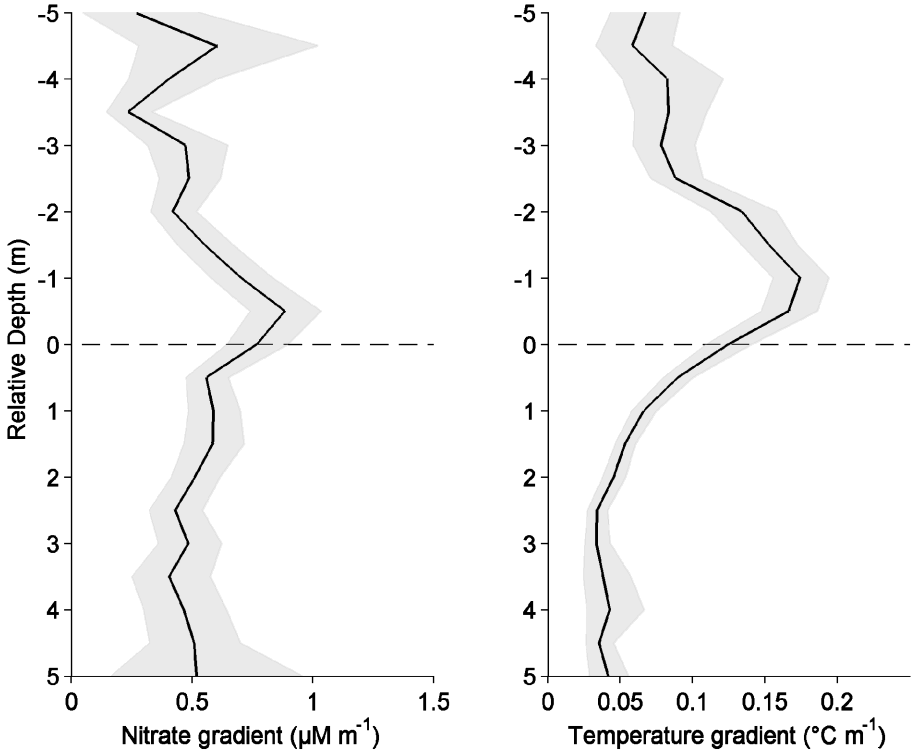

Figure 9 Nitrate and temperature gradient of all thin layers in Monterey Bay. Depth is relative to the center of thin layers, with negative values above and positive values below.

In both regions, the majority of thin layers are located inside the pycnocline. For those that are located outside the pycnocline, they are found mostly below the pycnocline in Monterey Bay (15%) and above the pycnocline in LSLE (12%), explaining the difference in the average position of thin layers, as shown in Figure 10. Despite the high Ri values, vertical shear was also highest at the center of thin layers, $S = 2.3 \times 10^{-2}\, s^{-1}$ (Figure 8). Shear can be associated with vertical gradients of current magnitude and/or rotation of currents with depth. To separate both effects, we decomposed shear into

$$S = \sqrt{S_M^2 + S_\theta^2}\,, \tag{4}$$

where S_M (s^{-1}) is the shear contribution due to change of current magnitude with depth given by :

$$S_M(z) = \left(\frac{\sqrt{u^2_{\left(z-\frac{\Delta z}{2}\right)} + v^2_{\left(z-\frac{\Delta z}{2}\right)}} - \sqrt{u^2_{\left(z+\frac{\Delta z}{2}\right)} + v^2_{\left(z+\frac{\Delta z}{2}\right)}}}{\Delta z} \right), \tag{5}$$

and S_θ (s^{-1}) is the shear contribution due to change of current direction with depth calculated with:

$$S_\theta(z) = \sqrt{2\left(\sqrt{\left(u^2_{\left(z-\frac{\Delta z}{2}\right)} + v^2_{\left(z-\frac{\Delta z}{2}\right)}\right)\left(u^2_{\left(z+\frac{\Delta z}{2}\right)} + v^2_{\left(z+\frac{\Delta z}{2}\right)}\right)} - \left(u_{\left(z-\frac{\Delta z}{2}\right)} u_{\left(z+\frac{\Delta z}{2}\right)} + v_{\left(z-\frac{\Delta z}{2}\right)} v_{\left(z+\frac{\Delta z}{2}\right)}\right)\right)}, \tag{6}$$

The total vertical shear was mainly explained by changes in the direction of the current as a function of depth, S_θ (Figure 8). Indeed, S_θ was maximum and approximately twice greater than S_M at the center of thin layers. Nevertheless, no correlation was found between shear and both thickness and intensity of thin layers in the LSLE.

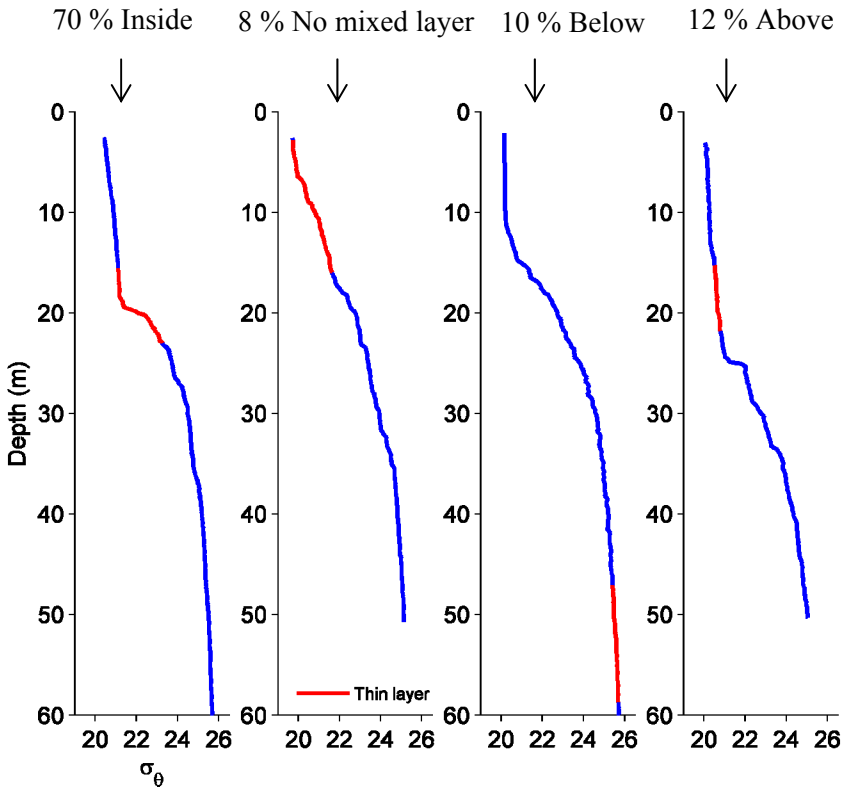

Figure 10 Thin layers location compared to the pycnocline in the LSLE and in Monterey Bay.

1.3.3 Frontal areas

The presence of frontal areas influenced the water column dynamics in both regions. Wind was one of the factors implicated in the development of fronts. In the LSLE, winds shifted from northeasterly to southwesterly on 16 May 2013 (Figure 11). Fronts were observed in this region however the strong stratification limited the impact of wind stress in the water column. In Monterey Bay wind was linked to the presence of fronts. In Monterey Bay, westerly winds were dominant at the LML wind station and there was a strong diurnal seabreeze signal with a velocity up to 10 m s^{-1} during the entire mission (Figure 11 b). The sea surface temperature showed an important evolution between 15 and 16 August (Figure 12).

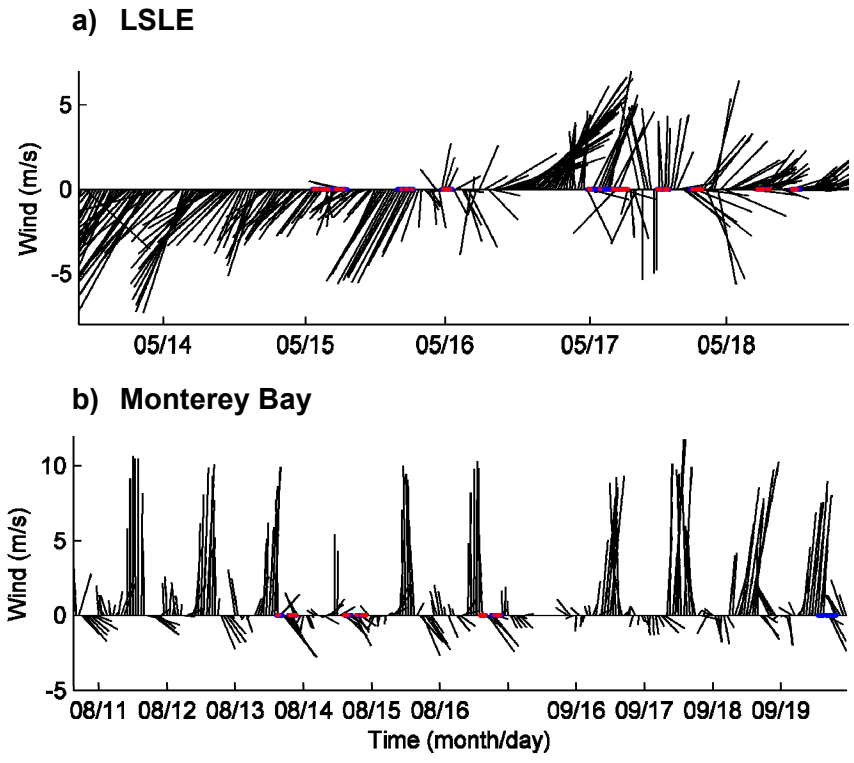

Figure 11 Time series of wind. a) North is oriented to the top and a one hour moving average filter was used. b) North is oriented to the left with hourly data. Blue points represent profiles and red points are profiles with thin layers.

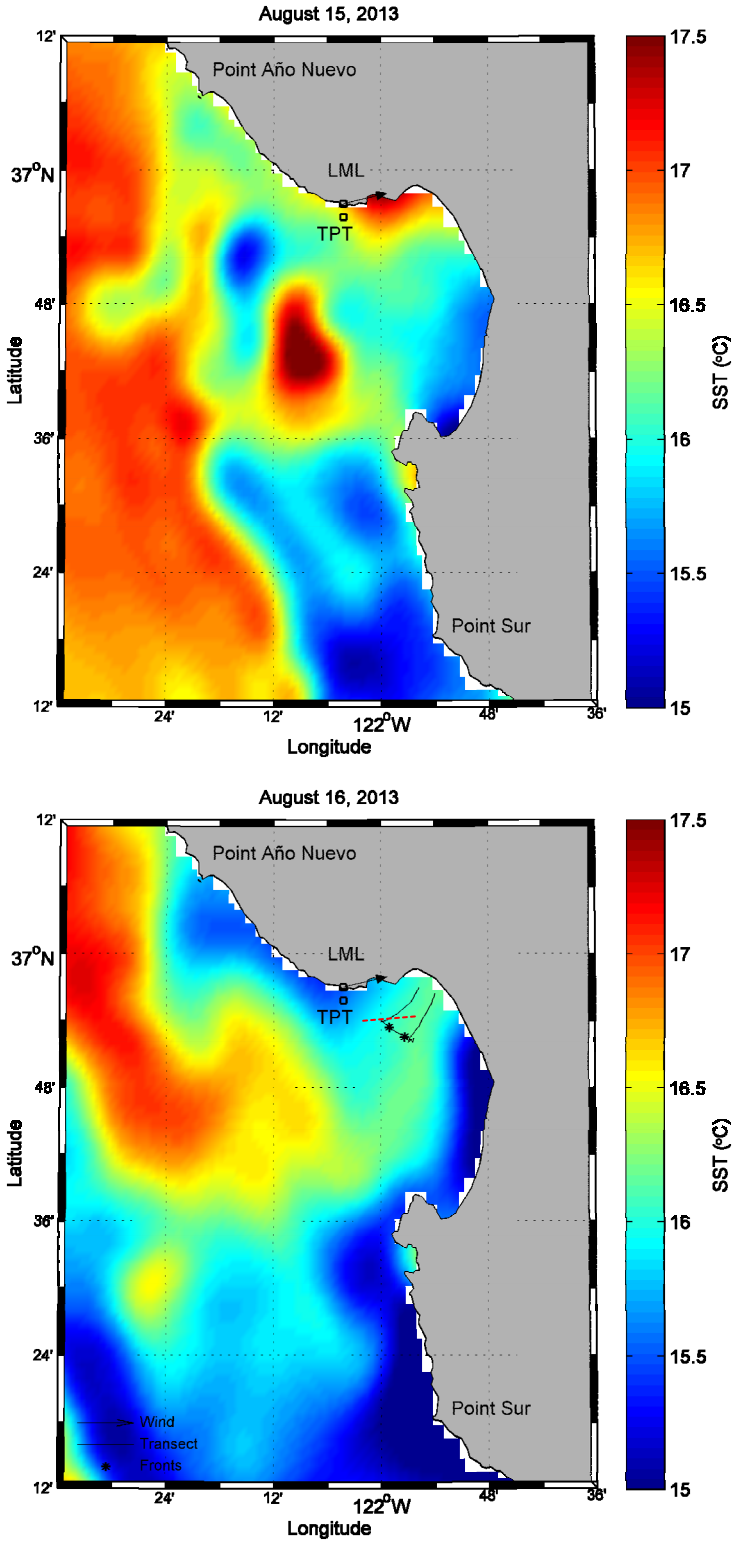

Figure 12 Map of the sea surface temperature on 15 and 16 August. Daily average wind velocity was 3 ms^{-1} and 3.3 ms^{-1} on August, 15 and 16, respectively. The red dashed line separates parts 1 and 2 of transect.

The warm water (up to 17.5°C) in the northeast of the bay was replaced by colder water (ca. 16°C) on 16 August. This was possibly due to the low wind the 14 August and to the upwelling-favorable westerly winds along the coast after this day (Figure 11 b). Fronts were found in two transects and only one of them is shown (Figure 13 Figure 14).

In Monterey Bay, fluorescence was concentrated at the thermocline most of the time. In Figure 13, high values of optical backscatter corresponded to high values of fluorescence, indicating that fluorescence maxima corresponded to biomass maxima in this region. Two patterns were observed in this transect. Between 10 km and 14 km, stratification was weak (Figure 14), and the fluorescence patch was diffuse.

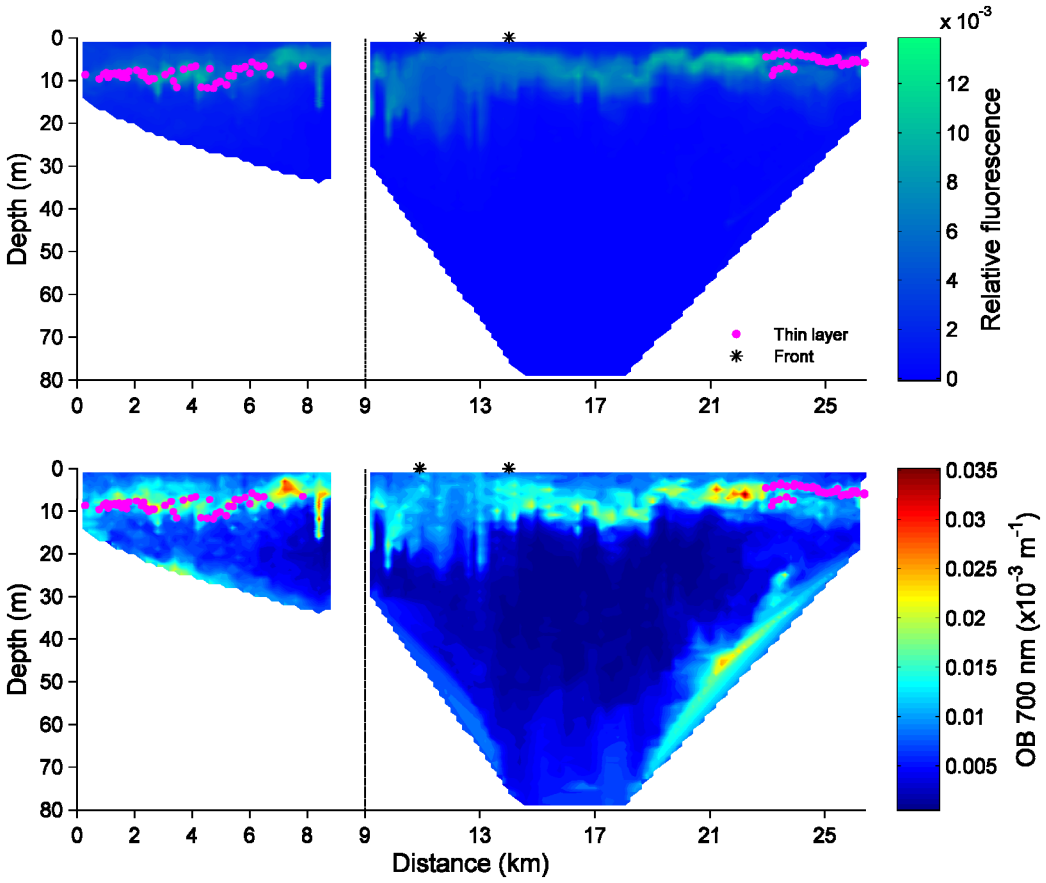

Figure 13 Relative fluorescence and optical backscattering were measured on 16 August 2013. The transect was performed in two parts with a 1 hour break between the parts. The black line marks the delimitation between these two parts. The stars show the location of the front's center. Magenta dots show thin layers.

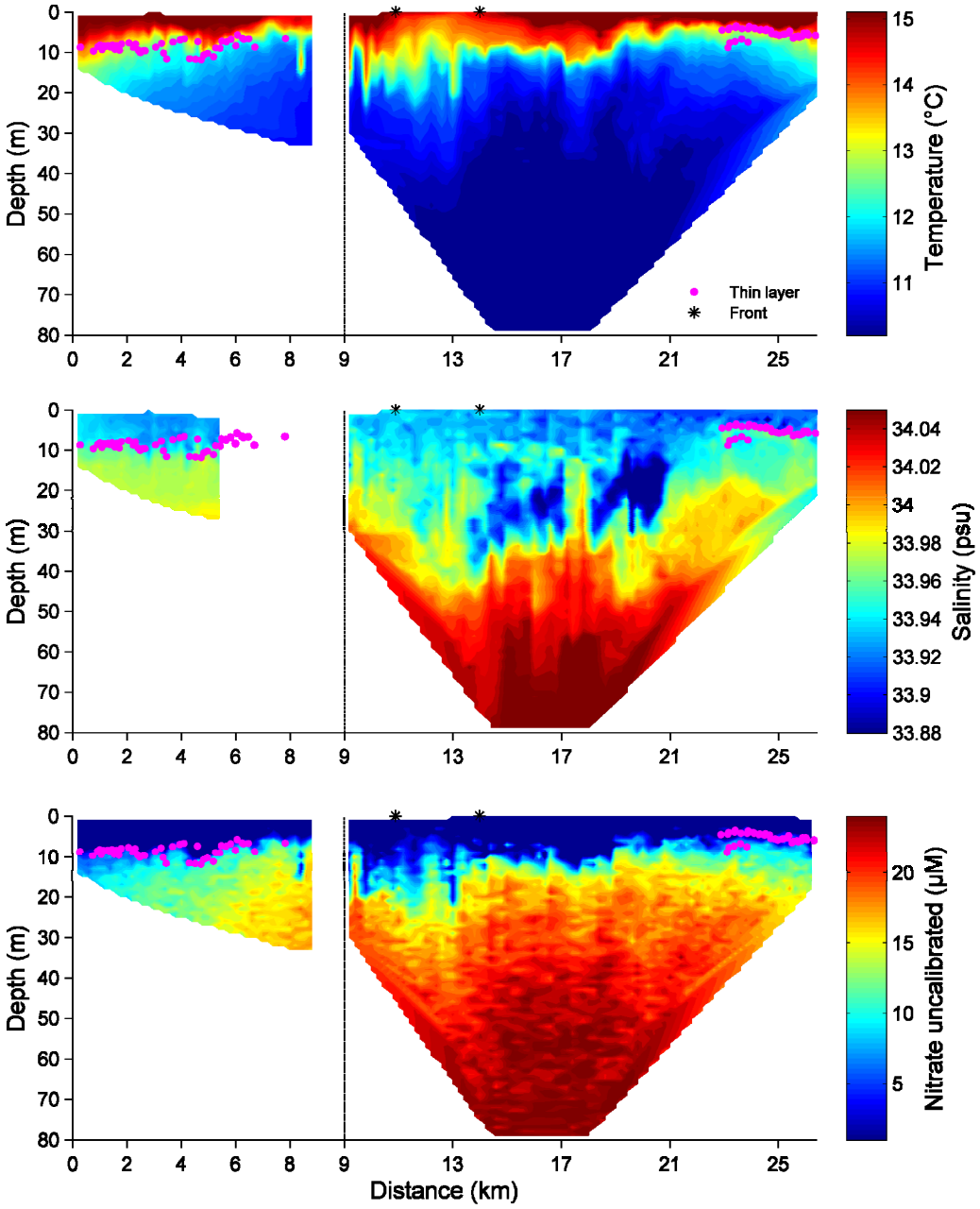

Figure 14 Temperature, salinity and uncalibrated nitrate concentration measured on 16 August 2013. Salinity data was missing at the end of the first part of transect due to a measurement problem. The stars show the location of the front's center. Magenta dots show thin layers.

On the other side of the front, from the beginning to 10 km and from 14 km to the end of transect, the stratification increased and the fluorescence patch was less diffuse, more intense and located in the thermocline (Figure 13 Figure 14). Starting at 19 km the fluorescence patch at the surface was progressively divided in two thinner and weaker fluorescence filaments. In each filament, there was a formation of thin layers (Figure 13). Those found in the filament located in the pycnocline were persistent over a distance of 3 km. Thin layers in the other filament, located below the pycnocline, were persistent only over 700 m. Moreover, from the beginning of transect to 8 km, a continuous thin layer was observed.

Fronts were observed in the majority of transects during the LSLE mission. A striking effect of fronts on phytoplankton distribution is illustrated in Figure 15. Fronts were located where isopycnals reached the surface, which corresponded to sea surface temperature gradients (Figure 15a, b). Although most of thin layers were located in or above the pycnocline in this transect (Figure 15c), some were observed between 40 m and 60 m depth in others transects and fixed stations (Figure 16a). The location of relatively warm temperature (2-3°C) below the pycnocline around 15 km and 63 km from the beginning of transect (Figure 15c) suggests that phytoplankton biomass which accumulated in surface water was displaced downward in the water column. Furthermore, the high photochemical quantum yield measured at the end of this transect during a fixed station (Figure 16d) indicates that phytoplankton had appropriate conditions for photosynthesis at 40 m and 60 m depth, despite the lack of photosynthetic available radiation (PAR) at these depths (Therriault and Levasseur 1985). This supports the hypothesis that these waters had been downwelled rapidly and recently. Thin layers were not confined to regions with high nitrate concentrations (Figure 16a, c). The occurrence of thin layers according to their distance from the fronts is shown in Figure 17 for all transects containing fronts realized during the LSLE mission. The number of profiles with thin layers decreases with increasing distance to the fronts but this is due to a sampling bias since more profiles were obtained near the fronts (Figure 17). Once normalized by the total number of profiles, the occurrence of thin layers was independent of the distance to the fronts.

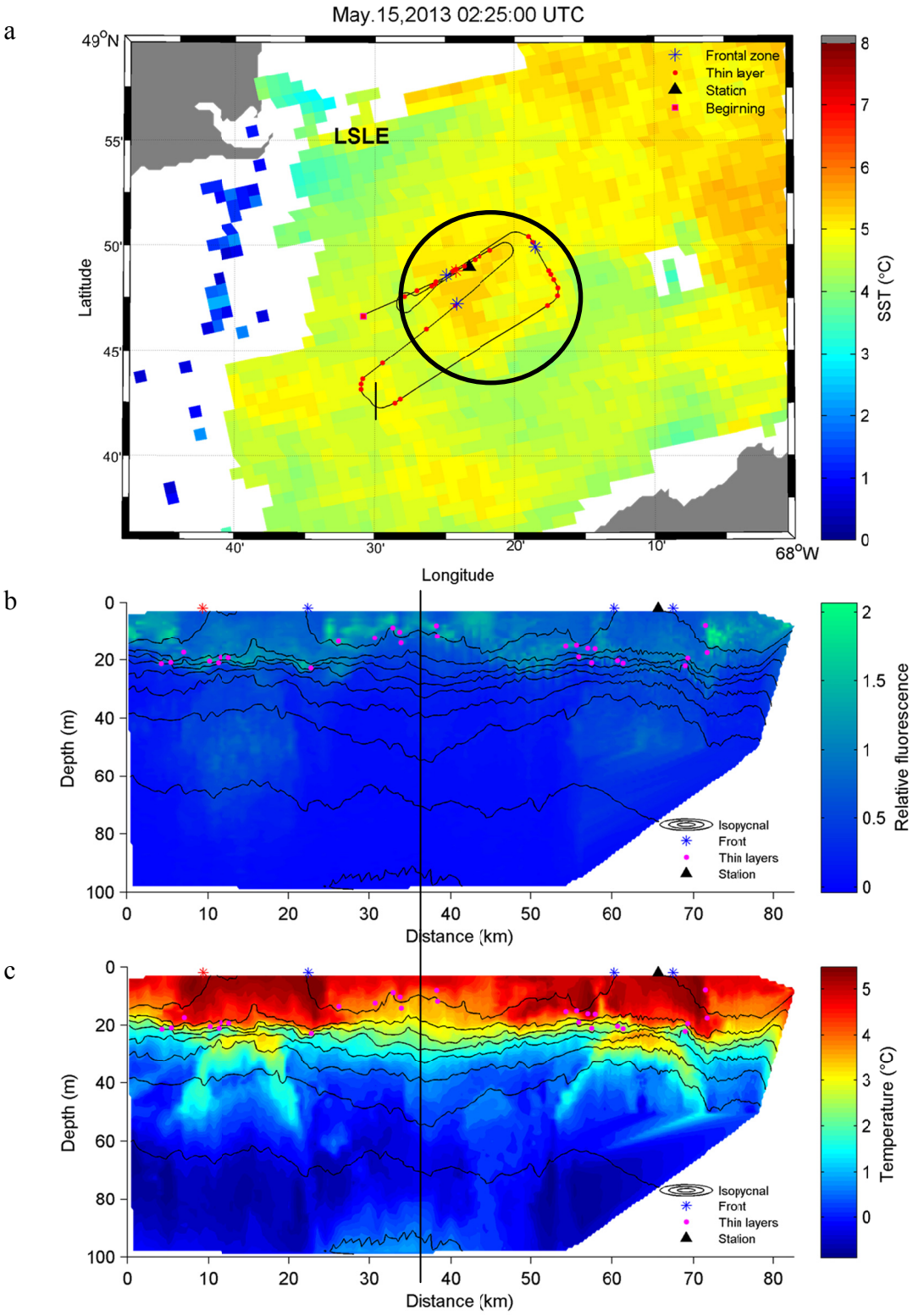

Figure 15 a) Map of the sea surface temperature in the LSLE, where black circle surrounds frontal zone, b) relative fluorescence and c) temperature measured during transect. The vertical line represents the return trip. The first star is red to help localize it. A fixed station was realized after the transect.

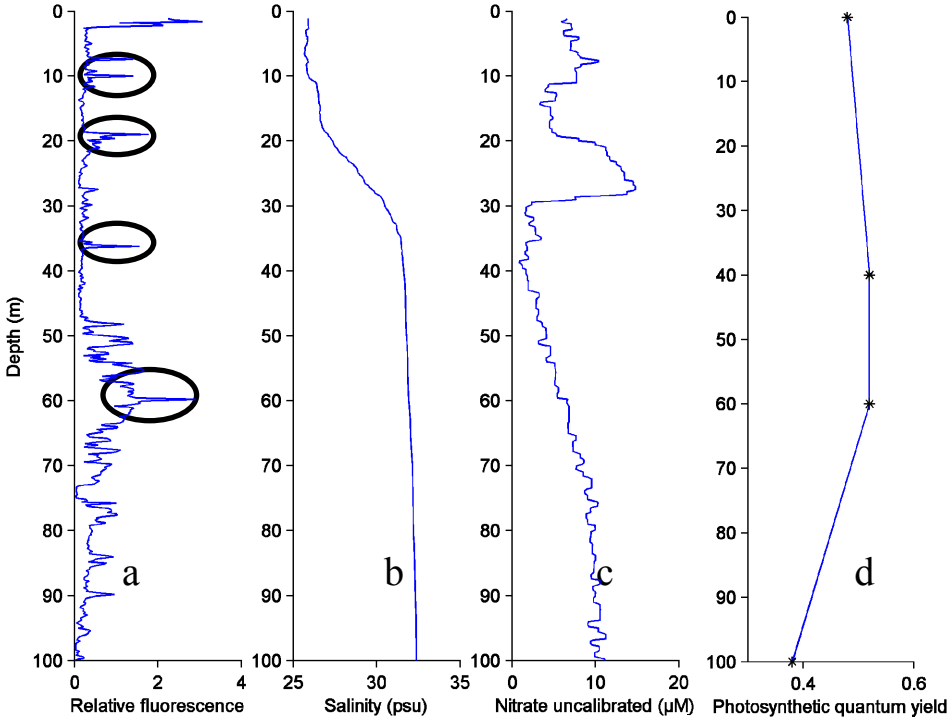

Figure 16 Variables measured during a fixed station at the end of transect of Figure 15. Black ellipses indicate the position of thin layers.

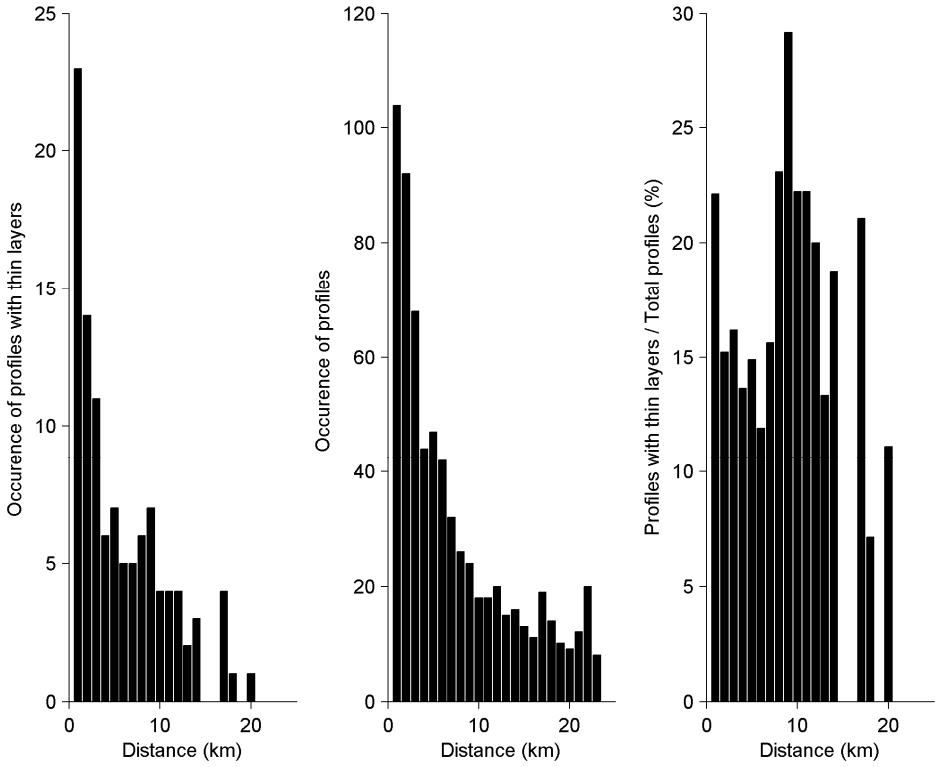

Figure 17 Relation between occurrence of thin layers and their distance to the center of fronts in the LSLE dataset.

According to the normalized occurrence of thin layers the region between 9 and 12 km from fronts appears to be favourable for thin layers (Figure 17) but this is probably not statistically significant due to the limited number of profiles.

1.3.4 Turbulent diffusion

One thin layer was detected in 19 casts during a fixed station in 2010 of the Transverse axis mission in the LSLE (Figure 18). The layer's position was above the pycnocline around 12 m depth. This location was probably explained by the high values of the dissipation rate of turbulent kinetic energy at the pycnocline. The values of dissipation rates were significantly lower in thin layers than in non-thin layers (Figure 18, right panel). The average dissipation rate inside thin layers was 2.6×10^{-9} W kg^{-1}. Moreover, except for some unusual values at the bottom of the layers, ε was lower than 10^{-7} W kg^{-1}.

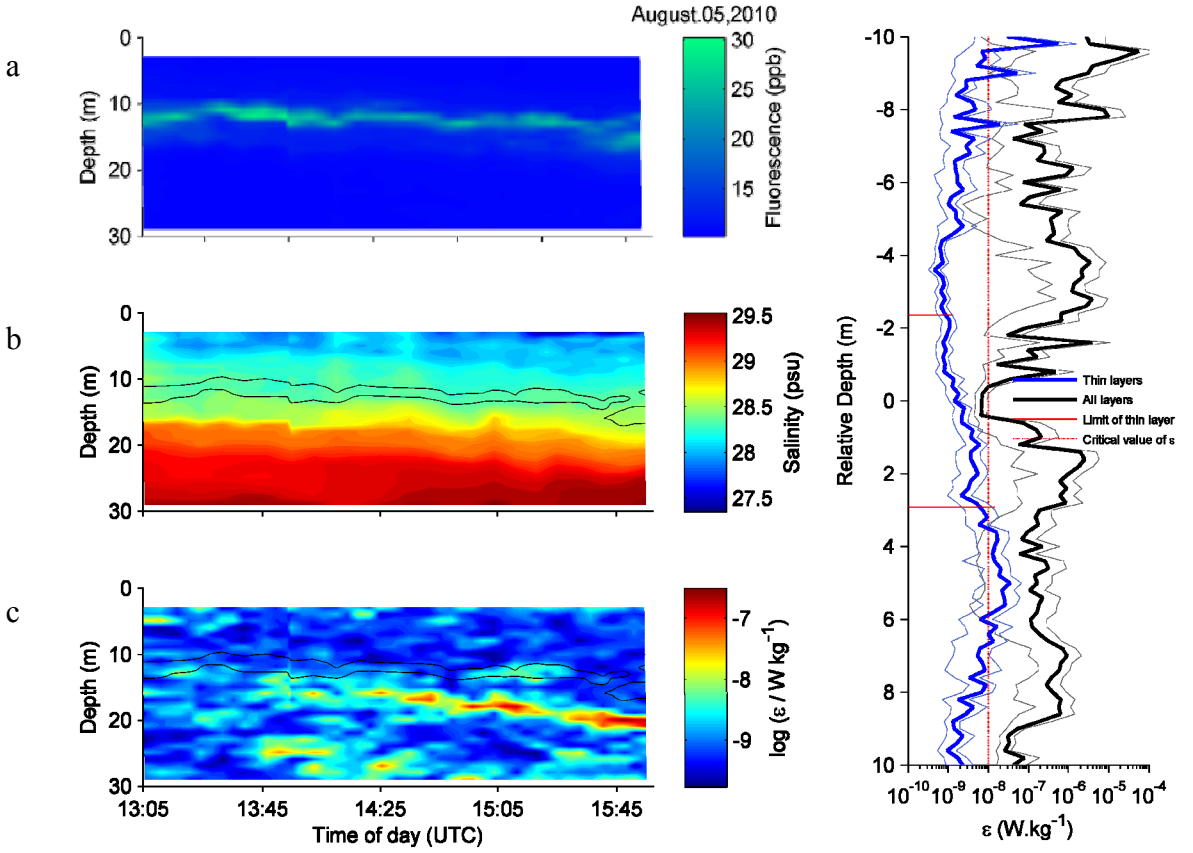

Figure 18 a) Fluorescence, b) salinity and c) dissipation rate of turbulent kinetic energy measured during a fixed station in the LSLE (Transverse axis dataset). Black lines show the thin layer contour. In the right panel, depth is relative to the center of thin layers, with negative values above and positive values below.

The wind can generate turbulence in the water column and affect the thickness of the surface mixing layer. Wind stress does not have the same effects on a stratified and unstratified water column. In this part we modelize the vertical mixing depth generated by the wind stress to compare it with the thin layers depth. According to Denman and Gargett (1983) and Kullenberg (1977), in an open ocean with a stratified fluid the length scale for the largest eddies is related to the buoyancy scale L_b (m):

$$L_b = \varepsilon^{\frac{1}{2}} N^{-\frac{3}{2}} \tag{7}$$

From Pingree et al. (1978) in the absence of any dissipation rate data, ε ($m^2 s^{-3}$) can be approximated by annex 1 :

$$\varepsilon = \frac{\rho_a}{\rho_w} \frac{C_{10}}{H} K_w U_{10}^3, \tag{8}$$

where ρ_w = 1025 kg m^{-3} and ρ_a = 1.2 kg m^{-3} are the water and air densities respectively, H (m) is the depth of the mixed layer, $C_{10} = 1.6 \times 10^{-3}$ is the drag coefficient for the wind at a height of 10 m, $K_w = 4 \times 10^{-2}$ is a wind correction factor for the wind generated surface current and U_{10} (m s^{-1}) is the wind speed at 10 m height. We assumed that H=L_b, which leads to the following expression:

$$L_b = \left(\frac{\rho a}{\rho w} C_{10} K_w \right)^{\frac{1}{3}} N^{-1} U_{10} \tag{9}$$

Instantaneous wind was used to calculate L_b for Monterey Bay and LSLE missions. Moreover, the mean buoyancy frequency of the active surface layer was used. The depth of the active surface mixing layer predicted by mechanical mixing parameterization was lower in LSLE than Monterey Bay for similar wind conditions, 4.9 m s-1 and 4 m s-1, then 0.7 m and 1.1 m respectively. This difference was mainly due to greater stratification near the surface. However, Lb is only a parameterization and can't perfectly represent the reality.

Tide affects vertical mixing in the water column. Two different tidal cycles were present during the missions in Monterey Bay. The first one was an unequal semi-diurnal tide during a neap to spring transition (13-16 August) where all transects contained thin layers. In contrast, the second one was an equal semi-diurnal tide during a spring to neap transition (19 September) where no thin layers were detected. The LSLE mission took place during a neap tidal period and thin layers were found at all phases of the semi-diurnal tidal cycle. Tides could have an effect on thin layers, but none have been demonstrated with our observations in both regions.

1.4 DISCUSSION

1.4.1 Distribution in both regions

The first aim of this work was to determine the presence of thin layers, their similarities and differences between Monterey Bay, the LSLE and the GSL. In the St. Lawrence, their frequency of occurrence was lower (between 1 % and 14 %) than in Monterey Bay (24 %). The frequency observed for Monterey Bay in the present work is consistent with values reported in the literature which vary from 15 % (Benoit-Bird et al. 2009) to 87 % (Sullivan et al. 2010). In the St. Lawrence, lower values may be explained by the timing of the sampling. The historical missions were realized during all seasons of the year except winter, while the LSLE mission was carried out in mid-May. However, the development of phytoplankton follows an annual cycle. In the GSL, blooms start in April-May, whereas there is a delay in the St. Lawrence Estuary where blooms occur in June before decreasing in September (Levasseur et al. 1984). This delay might be partly explained by the impossibility for the cells to accumulate in the mixed layer due to the high freshwater runoff and turbidity (Sinclair et al. 1981). Therefore, the frequency of occurrence of thin layers may be underestimated in the LSLE. In the GSL the annual frequency of occurrence was relatively lower than the frequency of occurrence measured during the summer (Figure 4). Moreover, the GSL's spatial sampling was not focusing on areas with high production of fluorescence / chlorophyll that could also underestimated the occurrence of thin layers, contrary to Monterey Bay. Concerning the thin layer's vertical distribution in the water column, there were two reasons to explain the difference for both regions (Figure 5). First, thin layers were observed near the surface in Monterey Bay because the pycnocline and the nutricline were closer to the surface compared to the St. Lawrence. Second, in the LSLE some thin layers were located down to 60 m possibly due to downwelling mechanisms.

1.4.2 Characterization of thin layers

It was possible to differentiate thin layers of both regions according to their spatial continuity. Churnside and Donaghay (2009) identified 2000 km of optical scattering layers in the Northeast Pacific and the Northeast Atlantic using an airborne LIDAR. They sorted them into 3 classes of thin layers. These classes showed different types of structures reflecting the different physical and/or chemical mechanisms acting on them. The first one corresponded to thin layers that were consistent and extended over kilometers. This may be due to aggregation of the phytoplankton along the nutricline for example. The second one represented a non-thin layer structure (which did not meet one of the three criteria) which became a thin layer in some places. This structure may be a consequence of the vertical shear. The last one corresponded to a non-thin layer structure, which was separated by a gap with a thin layer containing a lower fluorescence. This last structure can be the result of grazing by predators or other physical phenomena such as internal waves.

No thin layers belonged to the third class in both regions studied in this work. However, Monterey Bay had a bigger diversity of thin layers classes than the St. Lawrence. In the LSLE, there were only layers of the second class. In Figure 15, thin layers were present only in some locations in the non-thin layer structure. In Monterey Bay some layers belonged to the first class, such as the thin layer which extended continuously from the beginning of transect up to 8 km in Figure 13. A second class thin layer was also visible during the second part of the same transect. The fluorescence layer was large with low values at 10 km. Then, between 15 km and 23 km, the layer was thinner with higher values, before becoming a thin layer at 23 km (Figure 13).

1.4.3 Influence of physical, biological and chemical processes

The second major objective of this study was to examine the physical, biological, and chemical processes acting on thin layers in both locations. Our results showed that

downwelling mechanism, vertical shear, density stratification and turbulent diffusion were the essential elements affecting thin layers in the St. Lawrence. In Monterey Bay these essential elements were nutrients and density stratification.

1.4.3.1. The role of fronts

Frontal areas were observed in both regions and they probably induced different mechanisms acting on thin layers. In the LSLE, a downwelling which entrained phytoplanktonic cells was clearly identified with the pattern of temperature shown in Figure 15. Two elements support this interpretation. The first one was the dominance of non-motile species, e.g. *Thalassiosira nordenskioeldii*, in the deep water samples of this mission, at 45 and 100 m during fixed stations. These diatoms are common species in the LSLE (Levasseur et al. 1984, 1992; Roy et al. 1996; Savenkoff et al. 1997). The second one is the indication of rapid downwelling near-surface water to explain the high values of photochemical quantum yield of phytoplankton (Figure 16) measured at 40 m and 60 m, below the euphotic depth. In other transects (not shown) the fluorescence layer was also associated with an isopycnal sinking and thin layers were found at 54 m. Thin layers at this depth were persistent during a short time due to the absence of light (Therriault and Levasseur 1985). Furthermore, they were visible on different profiles and were likely due to an intrusion mechanism, during frontal processes. Intrusion processes of nutrient or phytoplankton rich waters into adjacent waters have already been shown their capacities to form thin layers (Kasai et al. 2010; Steinbuck et al. 2010). In other case, the low light and the nutrients could not permit the development of phytoplankton at this depth. Due to the advection mechanism, it was the only time that thin layers were located under the pycnocline in the LSLE. Another region in the LSLE is favourable to advection and intrusion mechanisms, the head of the Laurentian Channel (Gratton et al. 1988; Cyr and Larouche 2015). Due to its topography and to tidal mixing, the deep nutrient rich waters rise to the surface. In view of our observations and because it has a high concentration of chl a (Cyr and Larouche 2015), this region deserves attention for the study of thin layers in the future.

Fronts are also common in Monterey Bay. Graham (1993) had already described the northeast of the bay as a retention zone called the “upwelling shadow”. The mountainous topography of this region protects this part of the bay from high winds. This has multiple consequences such as decreased mixing. Consequently the stratification increases with warmer surface waters (Figure 14) (Graham 1993; Graham and Largier 1997). Wind had two effects in this region. The first one was to create a surface mixed layer and the second one was to induce the formation of fronts. Fronts were formed between 15 and 16 August 2013. As observed in the sea surface temperature field (Figure 12) changes in the wind regime, like the diurnal sea breeze (Figure 11), can cause temperature fluctuations of 2°C in the first 20 m of the surface (Woodson et al. 2007). Moreover for westerly winds, Ekman transport would be southward along the northern coast of the bay (offshore), which can cause local upwelling at Point Año Nuevo (Graham 1993). The eastward wind velocity was up to 10 m s^{-1} (Figure 11), sufficient to initiate equatorward movement of a front (Graham and Largier 1997; Woodson et al. 2009). The confluence between warm stratified waters of the bay and colder upwelled water produces fronts (Woodson et al. 2009).

The circulation at frontal zones is strongly vertically sheared. Vertical shear is known to form thin layers by spreading a patch of phytoplankton (Ryan et al. 2008; Durham et al. 2009). The vertical density stratification, limits or offsets the effect of turbulent diffusion (Stacey et al. 2007; Birch et al. 2008). In view of our observations we hypothesize that the vertical shear mechanism acted on thin layers. First, in the LSLE thin layers were located at local maxima of vertical shear, 2.3×10^{-2} s^{-1}. Secondly, this mechanism cannot increase the fluorescence values inside thin layers compared to surrounding water. This may explain why thin layers of the LSLE missions had generally the same magnitude than non-thin layers (Figure 6). Moreover, shear is also one of the typical formation mechanisms that can induce the class 2 thin layers met in the St. Lawrence (Churnside and Donaghay 2009). The low resolution of the vertical shear (4m) could probably explain the lack of correlation between the shear and the intensity and the thickness of thin layers. Our observations were coherent with other studies. Dekshenieks et al. (2001) observed 71 % of thin layers at the base of the pycnocline with a vertical shear comprised between 3×10^{-3} s^{-1} and 8.8×10^{-2} s^{-}

[1]. In the LSLE, 70 % of thin layers were located in the pycnocline with local maxima of stratification and Richardson number, 5.08×10^{-2} s^{-1}, 36.4 respectively (Figure 8). Other layers were always located in a stable environment with Ri> 0.25. In Monterey Bay the same observations of shear has already been mentioned by Ryan et al. (2008). In their study, the shear maximum, 2.2×10^{-2} s^{-1}, corresponded with the center of thin layers. Furthermore shear was associated with changes in the direction of horizontal currents, S_θ, similarly to our observations in the LSLE (Figure 8). Depending on the shape of the phytoplankton patch, the shear contribution due to change of current magnitude, S_M, and the shear contribution due to change of current direction, S_θ, can create thin layers with a different timing. In both cases the thickness of thin layers will be weaker than the original patch. If there is a vertical shear along a patch, before stretching this patch, it will be necessary for the shear to act during a longer time than the time required to displace the patch's original length. However, if the shear is caused by a change of current direction it can rapidly separate a phytoplankton patch in two thin layers, Figure 19. In this way, the rotational shear increases the chance to stretch the patch across its width. S_θ could be one of the mechanisms explaining the spatial discontinuity of thin layers observed in the LSLE (Figure 15). Indeed, it would be useful to have data of thin layers in 3D to confirm the effect of S_θ. In Monterey Bay, at the end of 16 August transect the layer of fluorescence was divided in two weaker and thinner thin layers (Figure 13). Thin layers that were located at the pycnocline were maintained longer than other thin layers located below the pycnocline. This observation could be the consequence of S_θ but no measurements of the vertical shear were realized during the Monterey Bay missions to confirm this hypothesis.

1.4.3.2. Turbulence: a divergence mechanism for the destruction of thin layers

Strong turbulence is known to erode thin layers (Stacey et al. 2007; Steinbuck et al. 2009; Durham et al. 2009). In the St. Lawrence, data from the transverse axis mission seems to support this statement.

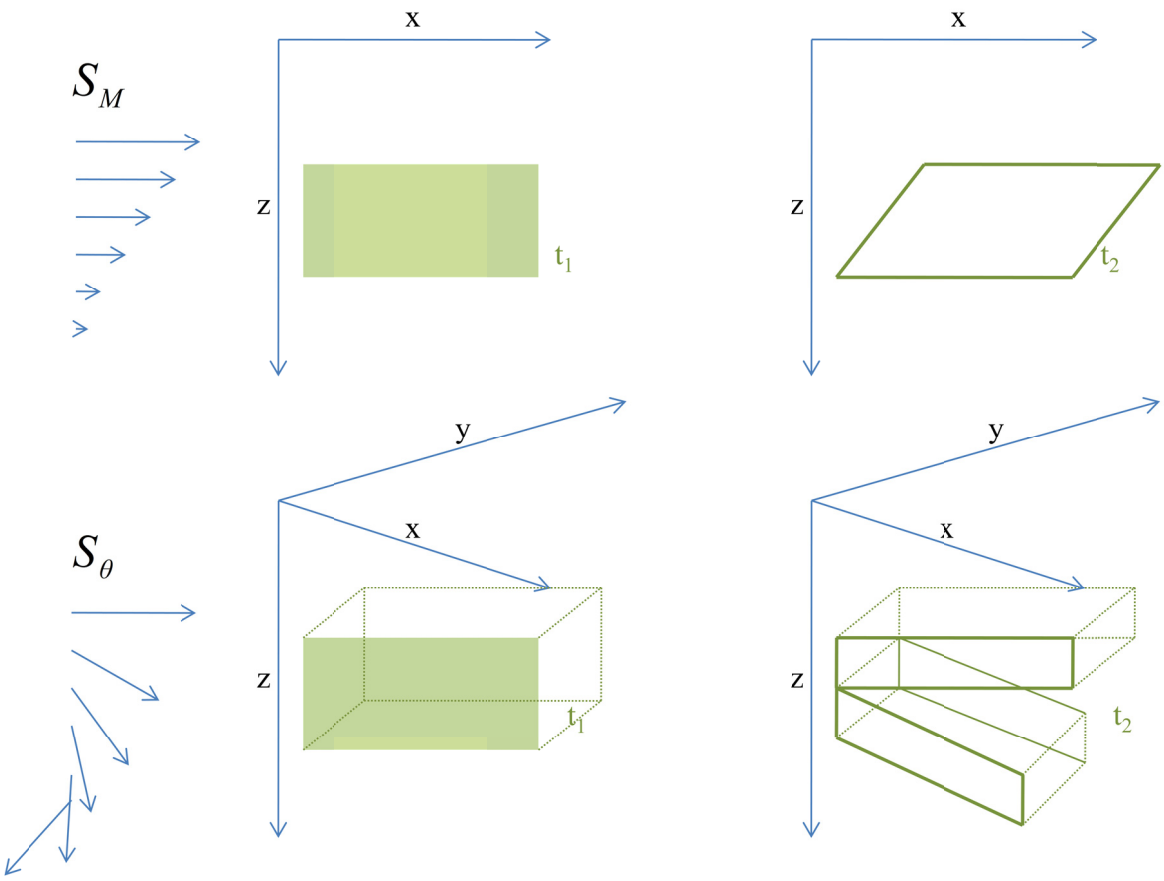

Figure 19 Both effects of the vertical shear on a phytoplankton patch.

Indeed, the high values of ε observed below the thin layer were responsible for its asymmetric shape (Figure 18); the fluorescence maximum was slightly closer to the top of the layer and the bottom tended to be diffused by turbulence. The thickness of the thin layer was explained partly by low values of dissipation rate inside this layer (2.6×10^{-9} W kg^{-1}), in comparison with non-thin layers (6.2×10^{-7} W kg^{-1}). Stacey et al. (2007) also analyzed the diffusive effect of turbulence inside thin layers from the study of Dekshenieks et al. (2001) and found that ε varied from 5×10^{-8} to 10^{-7} W kg^{-1}. Our observations were consistent with this study. This suggests that thin layers cannot survive in highly turbulent conditions.

Although no correlation was found between thin layers characteristics and L_b, the wind stress influenced the surface mixing depth in a manner that depends on its speed, its persistence (duration) and the stratification of the fluid. In both regions, the combination of the low wind and the stratification acted as a barrier for mixing, and turbulence induced by wind was limited to the first few meters below the surface. In Monterey Bay Drake et al. (2005) showed a coherence between winds from LML station and top temperature (4 m depth) from the mooring called Terrace Point (TPT) (Figure 12). During spring they found a maximum correlation (r = 0.68) in the temperature response to the wind stress with a 14 h lag. This correlation was limited in the immediate area of LML, and varied through the season. This delay and our parameterization of the surface mixing layer induced by the wind could underestimate L_b. We supposed that the wind can generates a degree of turbulence in the surface layer too high for the development of thin layers, which means that they are mostly found in the pycnocline.

1.4.3.3. Two different dynamics

Due to the strong vertical mixing at the head of the Laurentian Channel, nutrients are abundant throughout the whole year in the LSLE (Levasseur et al. 1984). Although some species, e.g. *Alexandrium tamarense*, can realize vertical migrations to optimize the conditions for their development (Fauchot et al. 2005), nutrients are considered not limiting for the growth of phytoplankton in the mixed layer (Sinclair et al. 1981; Levasseur et al. 1983). As observed in Figure 16 nitrate did not limit the development of four thin layers in this particular location. However nutrient dynamics are different between the LSLE and the north of Monterey Bay. During the upwelling season, nutrient concentrations are high and primary production is elevated inside Monterey Bay. Phytoplankton persistence in the north of the Bay depends on the supply of these nutrient-rich waters (Pennington and Chavez 2000). Thin layers were usually found in the nitracline (Figure 9). This was due to the lowest nitrate concentration near the surface (Figure 14).Indeed nitrate in the surface mixed layer during this period is generally under 1 μmol L^{-1} while the concentration can increase up to 13 μmol L^{-1} between 20-30 m depth (Steinbuck et al. 2009).

The presence of thin layers in the nitracline could explain the spatially coherent structure over kilometers of the class 1 thin layers (Churnside and Donaghay 2009). We hypothesize that phytoplankton must be motile to follow the displacement of the nitracline instead of the pycnocline from the beginning to the fifth kilometer of the 16 August transect. This hypothesis is supported by the dominance of dinoflagellates inside thin layers in Monterey Bay (McManus et al. 2008; Woodson et al. 2009; Rines et al. 2010). This species dominance is the consequence of a shift which appeared in 2004 (Jester et al. 2009). Downward migrations to the nitracline have already been observed (Ryan et al. 2010) as well as the swimming of dinoflagellates, *Akashiwo sanguinea*, found in thin layers (Steinbuck et al. 2009). As mentioned by Steinbuck et al. (2009), cell sinking of *A. Sanguinea* can not produce an upward velocity to maintain the thin layer. To explain the greater intensity of thin layers than non-thin layers structures in Monterey Bay, Figure 6, we hypothesize .that it's a question of time and nutrient; with more time, non-thin layers located in the nitracline could use nutrients to develop, before becoming a thin layer.

1.5 CONCLUSION

The aim of this study was to characterize thin layers and to determine the mechanisms acting on them in the St. Lawrence and Monterey Bay. For the first time, thin layers were observed in the Gulf and the Estuary of the St. Lawrence. The intensity and the thickness of thin layers were relatively the same between the two regions. Their intensity was greater than non-thin layers in both regions. Moreover, the frequency of occurrence up to 24 % in Monterey Bay was higher than in the St. Lawrence. The majority of thin layers were found in the pycnocline in the two regions. In the LSLE the principal mechanisms acting on thin layers were the vertical shear, with a maximum value equal to 2.3×10^{-2} s^{-1} at the center of thin layers, and intrusion processes. Thin layers need stable water conditions to develop and persist (Ri> 0.25) and low values of dissipation rate of the turbulent kinetic energy $\varepsilon = 2.6 \times 10^{-9}$ W kg^{-1} was measured inside a thin layer in the LSLE. This supports the existence of a threshold beyond which thin layers are not observed. In Monterey Bay, thin layers were usually located in the nitracline which was mostly located in the pycnocline. The wind stress induced a surface mixing layer that may impede the thin layers to develop.

Thin layers should clearly be considered as part of the ecosystem dynamics. In the St. Lawrence, species present inside thin layers are unknown whereas some harmful algal blooms have already been observed in Monterey Bay (McManus et al., 2008). With the new generation of instruments, multidisciplinary observations should become easier. Given our observations, we recommend continuing the study of thin layers in the St. Lawrence. This study has shown that the LSLE has all the necessary ingredients for the development of thin layers particularly at the head of the Laurentian channel.

Indeed, in this region during the bloom period, there is a high phytoplankton production associated with intrusion and advection mechanisms of nutrient rich waters. For the sampling, a better timing with the bloom period may increase the frequency of occurrence of thin layers. Sampling should also couple biological, chemical and physical

measurements. Predicting the development of thin layers requires the comprehension of phytoplankton ecology and of their interaction with the environment.

CONCLUSION GÉNÉRALE

Cette étude examine la présence des couches minces phytoplanctoniques et les mécanismes qui gouvernent leur dynamique dans deux environnements côtiers différents, l'Estuaire et le Golfe du Saint-Laurent et la baie de Monterey. Nos résultats confirment le caractère régulier des couches minces dans la Baie de Monterey avec une fréquence d'occurrence de l'ordre de 25 %. De plus, pour la première fois, des couches minces ont été répertoriées à l'intérieur du Golfe et de l'Estuaire du Saint-Laurent. Les fréquences d'occurrence observées dans ces zones étaient plus faibles, entre 1 % et 14%, soulignant ainsi l'hétérogénéité spatiale du phytoplancton. Grâce aux nombreuses variables physiques, biologiques et chimiques mesurées durant ces missions, il a été possible d'émettre certaines hypothèses quant aux mécanismes gouvernant la dynamique des couches minces. La présence d'une zone stable et peu turbulente était un critère important pour assurer le développement et/ou le maintien de ces dernières. Cela s'est traduit par la localisation de 70 % et 77 % des couches minces dans la pycnocline, respectivement dans l'EMSL et dans la Baie de Monterey.

Dans l'EMSL la circulation induite par les zones frontales pourrait engendrer l'apparition de mécanismes de cisaillement vertical et d'intrusion tels que ceux mentionnés pour la formation des couches minces dans l'introduction générale (figure 1a, f). De plus, la nécessité d'avoir une faible turbulence pour le maintien de couches minces a pu être observée à partir de données *in situ,* dans l'Estuaire Maritime du Saint-Laurent*,* et modélisées dans les deux régions. La stratification et les faibles valeurs de vent lors des transects ont ainsi limité l'impact du vent sur la colonne d'eau dans les deux régions. Dans la Baie de Monterey, la profondeur de mélange induite par le vent fluctuée en fonction de son intensité de manière plus importante que dans le Saint-Laurent. Ainsi, la profondeur des couches minces, au niveau de la pycnocline, pourrait être liée à la taille de la couche de mélange induite par le vent. Dans cette région la majorité des couches minces étaient situées dans la nitracline et suivait son évolution spatiale. Parallèlement, la motilité du phytoplancton pourrait permettre le maintien de certaines couches minces lorsque celles-ci

ne suivent pas les mouvements de la pycnocline en restant dans la nitracline (figure 1b). Bien que n'ayant pas fait l'objet de mesures spécifiques, les données relevées suggéraient aussi l'implication du cisaillement vertical dans la formation de certaines couches minces.

Cette étude a donc permis de confirmer l'importance et le rôle clef joués par certains mécanismes sur les couches minces dans la Baie de Monterey. De plus, elle a permis d'élargir les connaissances actuelles en analysant la zone du Saint-Laurent jusqu'alors inexplorée dans l'étude des couches minces.

Maintenant que certaines conditions favorables au développement des couches minces sont connues dans le Saint-Laurent, nous recommandons de poursuivre leur étude. Pour ce faire, au vu de nos résultats et des études existantes dans ce domaine, il est possible d'établir quelques lignes directrices concernant leur analyse. Les études devraient se concentrer sur des zones stratifiées, si possible situées proche de zones frontales et non soumises à des mécanismes turbulents ou des instabilités, telles les instabilités de Kelvin-Helmholtz. Par ailleurs, l'échantillonnage devrait être réalisé préférentiellement durant les périodes de bloom phytoplanctonique. Dépendamment des objectifs d'études, différentes sondes ou types d'échantillonnage peuvent être utilisés. L'utilisation de la télédétection optique tel que le LIDAR aéroporté, est possible car les couches minces observées sont suffisamment épaisses (de l'ordre du mètre) et intenses pour être détectées. De plus la quasi-totalité était située dans la couche de surface. Cette technique est un bon compromis pour répondre à des questions concernant la continuité, la fréquence d'occurrence, les variations des couches minces soumises à différentes conditions environnementales sur de grandes échelles spatiales et temporelles. Cependant pour des études plus localisées, les aspects biologiques et écologiques devraient être étudiés prioritairement, aussi bien dans le Saint-Laurent et dans la Baie de Monterey que dans d'autres régions du globe.

En effet, les problématiques générales de l'écologie telles que les interactions entre les organismes (réponses, adaptations, impacts) présents dans les couches minces et ceux présents dans l'ensemble de l'écosystème, sont principalement abordées dans les cas extrêmes où les couches minces possèdent des algues toxiques. Dès lors, cet aspect moins

connu des couches minces devrait faire l'objet d'un plus grand nombre d'investigations. Néanmoins, ce type d'études soulève la question : quelle méthode d'échantillonnage faut-il utiliser ? La complexité de l'échantillonnage réside d'abord dans la synchronisation et la diversité du nombre de systèmes/sondes à utiliser, mais aussi dans la manière dont il est possible d'étudier ces interactions. Une chose est sûre, il y a nécessité d'effectuer des mesures et des prélèvements *in situ*. Pour ce faire, l'utilisation de véhicules autonomes sous-marins, comme celui utilisé dans cette étude, est particulièrement appropriée.

Annex 1

Derivation to obtain equation (2) from Pingree et al. (1978) using Kullenberg (1977)

- Energy input per unit time and area from wind :

$E = V_0 \tau_0$ where V_0 is the surface wind-generated current and τ_0 is the surface stress

Parameterizations: 1) $V_0 = KU_{10}$ where K is the wind factor and U_{10} is the wind speed at a height of 10 m.

2) $\tau 0 = \rho_a C_{10} U_{10}^2$ where ρ_a is the density of air and C_{10} is the drag coefficient for the wind at a height of 10 m.

$=> E = \rho_a C_{10} K U_{10}^3$

- Energy dissipation rate per unit mass due to wind mixing : ε

For steady state: $\int_{-H}^{0} \rho_w \varepsilon(z) dz = E$ where ρ_w is the density of sea water and H is the depth of the pycnocline

$=> \rho_w H \bar{\varepsilon} = \rho_a C_{10} K U_{10}^3$ where $\bar{\varepsilon} = \frac{1}{H} \int_{-H}^{0} \varepsilon(z) dz$

$=> \bar{\varepsilon} = \frac{\rho_a C_{10} K U_{10}^3}{\rho_w H}$ as (2) in Pingree et al. (1978)

RÉFÉRENCES BIBLIOGRAPHIQUES

Bainbridge, R. 1957. The size, shape and density of marine phytoplankton concentrations. Biol. Rev. **32**: 91–115.

Banks, R. E. 1966. The cold layer in the Gulf of St. Lawrence. J. Geophys. Res. **71**: 1603–1610.

Barber, R. T., and R. L. Smith. 1981. Coastal upwelling ecosystems, p. 31–68. *In* A.R. Longhurst [ed.], Analysis of Marine Ecosystems. Academic Press.

Benoit-Bird, K. J., T. J. Cowles, and C. E. Wingard. 2009. Edge gradients provide evidence of ecological interactions in planktonic thin layers. Limnol. Oceanogr. **54**: 1382–1392. doi:10.4319/lo.2009.54.4.1382

Birch, D. A., W. R. Young, and P. J. S. Franks. 2008. Thin layers of plankton: Formation by shear and death by diffusion. Deep. Res. Part I Oceanogr. Res. Pap. **55**: 277–295. doi:10.1016/j.dsr.2007.11.009

Bourgault, D., D. E. Kelley, and P. S. Galbraith. 2008. Turbulence and boluses on an internal beach. J. Mar. Res. **66**: 563–588.

Churnside, J. H., and P. L. Donaghay. 2009. Thin scattering layers observed by airborne lidar. ICES J. Mar. Sci. **66**: 778–789. doi:10.1093/icesjms/fsp029

Cyr, F., D. Bourgault, and P. S. Galbraith. 2011. Interior versus boundary mixing of a cold intermediate layer. J. Geophys. Res. Ocean. **116**: 1–12. doi:10.1029/2011JC007359

Cyr, F., D. Bourgault, P. S. Galbraith, and M. Gosselin. 2015. Turbulent nitrate fluxes in the Lower St. Lawrence Estuary, Canada. J. Geophys. Res. Ocean. **120**: 2308–2330. doi:10.1002/2014JC010272

Cyr, F., and P. Larouche. 2015. Thermal fronts atlas of Canadian coastal waters. Atmosphere-Ocean **53**: 212–236.

Dekshenieks, M., P. Donaghay, J. Sullivan, J. Rines, T. Osborn, and M. Twardowski. 2001. Temporal and spatial occurrence of thin phytoplankton layers in relation to physical processes. Mar. Ecol. Prog. Ser. **223**: 61–71.

Demers, S., and L. Legendre. 1981. Mélange vertical et capacité photosynthétique du phytoplancton estuarien (estuaire du Saint-Laurent). Mar. Biol. **250**: 243–250.

Denman, K. L., and A. E. Gargett. 1983. Time and space scales of vertical mixing and advection of phytoplankton in the upper ocean. Limnol. Oceanogr. **28**: 801–815.

Drake, P. T., M. A. McManus, and C. D. Storlazzi. 2005. Local wind forcing of the Monterey Bay area inner shelf. Cont. Shelf Res. **25**: 397–417.

doi:10.1016/j.csr.2004.10.006

Durham, W. M., J. O. Kessler, and R. Stocker. 2009. Disruption of vertical motility by shear triggers formation of thin phytoplankton layers. Science (80-.). **323**: 1067–70. doi:10.1126/science.1167334

Durham, W. M., and R. Stocker. 2012. Thin phytoplankton layers: characteristics, mechanisms, and consequences. Ann. Rev. Mar. Sci. **4**: 177–207. doi:10.1146/annurev-marine-120710-100957

Falkowski, P. G. 1994. The role of phytoplankton photosyntesis in global biogeochemical cycles. Photosynth. Res. **39**: 235–258.

Fauchot, J., M. Levasseur, and S. Roy. 2005. Daytime and nighttime vertical migrations of *Alexandrium tamarense* in the St. Lawrence estuary (Canada). Mar. Ecol. Prog. Ser. **296**: 241–250. doi:10.3354/meps296241

Gilbert, D., B. Sundby, C. Gobeil, A. Mucci, and G.-H. Tremblay. 2005. A seventy-two-year record of diminishing deep-water oxygen in the St. Lawrence estuary: The northwest Atlantic connection. Limnol. Oceanogr. **50**: 1654–1666. doi:10.4319/lo.2005.50.5.1654

Graham, W. M. 1993. Spatio-temporal scale assessment of an "upwelling shadow" in Northern Monterey Bay, California. Estuaries and Coasts **16**: 83–91.

Graham, W. M., and J. L. Largier. 1997. Upwelling shadows as nearshore retention sites: The example of northern Monterey Bay. Cont. Shelf Res. **17**: 509–532. doi:10.1016/S0278-4343(96)00045-3

Gratton, Y., G. Mertz, and J. A. Gagné. 1988. Satellite observations of tidal upwelling and mixing in the St. Lawrence Estuary. J. Geophys. Res. **93**: 6947–6954.

Haury, L. R., J. A. McGowan, and P. H. Wiebe. 1978. Patterns and processes in the time-space scales of plankton distributions, p. 277–327. *In* NATO Conference Series.

Hodges, B. A., and D. M. Fratantoni. 2009. A thin layer of phytoplankton observed in the Philippine Sea with a synthetic moored array of autonomous gliders. J. Geophys. Res. Ocean. **114**: 1–15. doi:10.1029/2009JC005317

Ingram, R., and M. El-Sabh. 1990. Fronts and mesoscale features in the St. Lawrence estuary., p. 71–93. *In* M. El-Sabh and N. Silverberg [eds.], Oceanography of a large scale estuarine system: The St. Lawrence. Springer-Verlag.

Jessup, D. A., M. A. Miller, J. P. Ryan, and others. 2009. Mass stranding of marine birds caused by a surfactant-producing red tide. PLoS One **4**. doi:10.1371/journal.pone.0004550

Jester, R., K. Lefebvre, G. Langlois, V. Vigilant, K. Baugh, and M. W. Silver. 2009. A shift in the dominant toxin-producing algal species in central California alters phycotoxins in food webs. Harmful Algae **8**: 291–298. doi:10.1016/j.hal.2008.07.001

Johnson, K. S., and L. J. Coletti. 2002. In situ ultraviolet spectrophotometry for high resolution and long-term monitoring of nitrate, bromide and bisulfide in the ocean. Deep. Res. Part I Oceanogr. Res. Pap. **49**: 1291–1305. doi:10.1016/S0967-0637(02)00020-1

Johnston, T., O. Cheriton, J. Pennington, and F. Chavez. 2009. Thin phytoplankton layer formation at eddies, filaments, and fronts in a coastal upwelling zone. Deep Sea Res. Part II Top. Stud. Oceanogr. **56**: 246–259.

Kasai, A., Y. Kurikawa, M. Ueno, D. Robert, and Y. Yamashita. 2010. Salt-wedge intrusion of seawater and its implication for phytoplankton dynamics in the Yura Estuary, Japan. Estuar. Coast. Shelf Sci. **86**: 408–414.

Koutitonsky, V. G., and G. L. Bugden. 1991. The physical oceanography of the Gulf of St. Lawrence: a review with emphasis on the synoptic variability of the motion, p. 57–90. *In* J.-C. Therriault [ed.], The Gulf of St. Lawrence: small ocean or big estuary ? Canadian Special Publication of Fisheries and Aquatic Sciences.

Kullenberg, G. 1977. Entrainment velocity in natural stratified vertical shear flow. Estuar. Coast. Mar. Sci. **5**: 329–338. doi:10.1016/0302-3524(77)90060-3

Levasseur, M., L. Fortier, J.-C. Therriault, and P. Harrison. 1992. Phytoplankton dynamics in a coastal jet frontal region. Mar. Ecol. Prog. Ser. **86**: 283–295. doi:10.3354/meps086283

Levasseur, M., J.-C. Therriault, and L. Legendre. 1983. Tidal currents, winds and the morphology of phytoplankton spatial structures. J. Mar. Res. **41**: 655–672. doi:10.1357/002224083788520450

Levasseur, M., J.-C. Therriault, and L. Legendre. 1984. Hierarchical control of phytoplankton succession by physical factors. Mar. Ecol. Prog. Ser. **19**: 211–222.

McManus, M. A., R. M. Kudela, M. W. Silver, G. F. Steward, P. L. Donaghay, and J. M. Sullivan. 2008. Cryptic blooms: are thin layers the missing connection? Estuaries and Coasts **31**: 396–401. doi:10.1007/s12237-007-9025-4

McManus, M., A. Alldredge, A. Barnard, and others. 2003. Characteristics, distribution and persistence of thin layers over a 48 hour period. Mar. Ecol. Prog. Ser. **261**: 1–19. doi:10.3354/meps261001

Mertz, G., and Y. Gratton. 1990. Topographic Waves and Topographically Induced Motions in the St. Lawrence Estuary, p. 94–108. *In* M.I. El-Sabh and N. Silverberg [eds.], Oceanography of a Large-Scale Estuarine System. Springer-Verlag.

Moline, M. A., K. J. Benoit-Bird, I. C. Robbins, M. Schroth-Miller, C. M. Waluk, and B. Zelenke. 2010. Integrated measurements of acoustical and optical thin layers II: Horizontal length scales. Cont. Shelf Res. **30**: 29–38. doi:10.1016/j.csr.2009.08.004

Pennington, J. T., and F. P. Chavez. 2000. Seasonal fluctuations of temperature, salinity, nitrate, chlorophyll and primary production at station H3 / M1 over 1989-1996 in Monterey Bay, California. Deep. Res. II **47**: 947–973.

Pingree, R. D., P. M. Holligan, and G. T. Mardelle. 1978. The effects of vertical stabiliy on phytoplankton distributions in the summer on the northwest European Shelf. Deep Sea Res. **25**: 1011–1028.

Rines, J. E. B., P. L. Donaghay, M. M. Dekshenieks, J. M. Sullivan, and M. S. Twardowski. 2002. Thin layers and camouflage: Hidden *Pseudo-nitzschia* spp. (Bacillariophyceae) populations in a fjord in the San Juan Islands, Washington, USA. Mar. Ecol. Prog. Ser. **225**: 123–137. doi:10.3354/meps225123

Rines, J. E. B., M. N. Mcfarland, P. L. Donaghay, and J. M. Sullivan. 2010. Thin layers and species-specific characterization of the phytoplankton community in Monterey Bay, California, USA. Cont. Shelf Res. **30**: 66–80. doi:10.1016/j.csr.2009.11.001

Rosenfeld, L. K., F. B. Schwing, N. Garfield, and D. E. Tracy. 1994. Bifurcated flow from an upwelling center: a cold water source for Monterey Bay. Cont. Shelf Res. **14**.

Roy, S., J. P. Chanut, M. Gosselin, and T. Sime-Ngando. 1996. Characterization of phytoplankton communities in the lower St. Lawrence Estuary using HPLC-detected pigments and cell microscopy. Mar. Ecol. Prog. Ser. **142**: 55–73. doi:10.3354/meps142055

Ryan, J. P., F. P. Chavez, and J. G. Bellingham. 2005. Physical-biological coupling in Monterey Bay, California: Topographic influences on phytoplankton ecology. Mar. Ecol. Prog. Ser. **287**: 23–32. doi:10.3354/meps287023

Ryan, J. P., A. M. Fischer, R. M. Kudela, J. F. R. Gower, S. A. King, R. Marin, and F. P. Chavez. 2009. Influences of upwelling and downwelling winds on red tide bloom dynamics in Monterey Bay, California. Cont. Shelf Res. **29**: 785–795. doi:10.1016/j.csr.2008.11.006

Ryan, J. P., M. A. McManus, J. D. Paduan, and F. P. Chavez. 2008. Phytoplankton thin layers caused by shear in frontal zones of a coastal upwelling system. Mar. Ecol. Prog. Ser. **354**: 21–34. doi:10.3354/meps07222

Ryan, J. P., M. A. McManus, and J. M. Sullivan. 2010. Interacting physical, chemical and biological forcing of phytoplankton thin-layer variability in Monterey Bay, California. Cont. Shelf Res. **30**: 7–16. doi:10.1016/j.csr.2009.10.017

Savenkoff, C., A. F. Vézina, and Y. Gratton. 1997. Effect of a freshwater pulse on

mesoscale circulation and phytoplankton distribution in the lower St. Lawrence Estuary. J. Mar. Res. **55**: 353–381. doi:10.1357/0022240973224445

Sinclair, M., D. V. S. Rao, and R. Couture. 1981. Phytoplankton temporal distributions in estuaries. Oceanol. Acta **4**: 239–246.

Skogsberg, T., and A. Phelps. 1946. Hydrography of Monterey Bay, California. Thermal Conditions, Part II (1934-1937). Am. Philos. Soc. **90**: 350–386. doi:10.1016/S0016-0032(38)92229-X

Smayda, T. J. 2002. Turbulence, watermass stratification and harmful algal blooms: An alternative view and frontal zones as "pelagic seed banks." Harmful Algae **1**: 95–112. doi:10.1016/S1568-9883(02)00010-0

Stacey, M. T., M. A. McManus, and J. V. Steinbuck. 2007. Convergences and divergences and thin layer formation and maintenance. Limnol. Oceanogr. **52**: 1523–1532. doi:10.4319/lo.2007.52.4.1523

Steinbuck, J. V., A. Genin, S. G. Monismith, J. R. Koseff, R. Holzman, and R. G. Labiosa. 2010. Turbulent mixing in fine-scale phytoplankton layers: observations and inferences of layer dynamics. Cont. Shelf Res. **30**: 442–455. doi:10.1016/j.csr.2009.12.014

Steinbuck, J. V., M. Stacey, M. A. McManus, O. Cheriton, and J. P. Ryan. 2009. Observations of turbulent mixing in a phytoplankton thin layer: implications for formation, maintenance, and breakdown. Limnol. Oceanogr. **54**: 1353–1368.

Strickland, J. D. H. 1968. A comparaison of profiles of nutrient and chlorophyll concentrations from discreet depth and by continuous recording. Limnol. Oceanogr. **13**: 388–391.

Strub, P. T., J. S. Allen, A. Huyer, R. L. Smith, and R. C. Beardsley. 1987. Seasonal cycles of currents, temperatures, winds, and sea level over the northeast Pacific continental shelf: 35°N to 48°N. J. Geophys. Res. **92**: 1507–1526. doi:10.1029/JC092iC02p01507

Sullivan, J. M., P. L. Donaghay, and J. E. B. Rines. 2010. Coastal thin layer dynamics: consequences to biology and optics. Cont. Shelf Res. **30**: 50–65. doi:10.1016/j.csr.2009.07.009

Sullivan, J. M., E. Swift, P. L. Donaghay, and J. E. B. Rines. 2003. Small-scale turbulence affects the division rate and morphology of two red-tide dinoflagellates. Harmful Algae **2**: 183–199. doi:10.1016/S1568-9883(03)00039-8

Therriault, J.-C., and M. Levasseur. 1985. Control of phytoplankton production in the lower St Lawrence estuary: light and freshwater runoff. Nat. Can. **112**: 77–96.

Vandevelde, T., L. Legendre, J.-C. Therriault, S. Demers, and A. Bah. 1987. Subsurface

chlorophyll maximum and hydrodynamics of the water column. J. Mar. Res. **45**: 377–396. doi:10.1357/002224087788401151

Vézina, A. F., Y. Gratton, and P. Vinet. 1995. Mesoscale physical-biological variability during a summer phytoplankton bloom in the lower St Lawrence estuary. Estuar. Coast. Shelf Sci. **41**: 393–411.

Wang, Z., and L. Goodman. 2010. The evolution of a thin phytoplankton layer in strong turbulence. Cont. Shelf Res. **30**: 104–118. doi:10.1016/j.csr.2009.08.006

White, A. E., Y. H. Spitz, and R. M. Letelier. 2006. Modeling carbohydrate ballasting by Trichodesmium spp. Mar. Ecol. Prog. Ser. **323**: 35–45. doi:10.3354/meps323035

Woodson, C. B., D. I. Eerkes-Medrano, A. Flores-Morales, and others. 2007. Local diurnal upwelling driven by sea breezes in northern Monterey Bay. Cont. Shelf Res. **27**: 2289–2302. doi:10.1016/j.csr.2007.05.014

Woodson, C. B., L. Washburn, J. A. Barth, D. J. Hoover, A. R. Kirincich, M. A. McManus, J. P. Ryan, and J. Tyburczy. 2009. Northern Monterey Bay upwelling shadow front: Observations of a coastally and surface-trapped buoyant plume. J. Geophys. Res. Ocean. **114**: 1–15. doi:10.1029/2009JC005623

Yamazaki, H., H. Honma, T. Nagai, M. J. Doubell, K. Amakasu, and M. Kumagai. 2010. Multilayer biological structure and mixing in the upper water column of Lake Biwa during summer 2008. Limnology **11**: 63–70. doi:10.1007/s10201-009-0288-2